

# Accepted Manuscript

Structure-activity studies on *N*-Substituted tranlycypromine derivatives lead to selective inhibitors of lysine specific demethylase 1 (LSD1) and potent inducers of leukemic cell differentiation

Johannes Schulz-Fincke, Mirjam Hau, Jessica Barth, Dina Robaa, Dominica Willmann, Andreas Kürner, Julian Haas, Gabriele Greve, Tinka Haydn, Simone Fulda, Michael Lübbert, Steffen Lüdeke, Tobias Berg, Wolfgang Sippl, Roland Schüle, Manfred Jung

PII: S0223-5234(17)31007-3

DOI: [10.1016/j.ejmech.2017.12.001](https://doi.org/10.1016/j.ejmech.2017.12.001)

Reference: EJMECH 9979

To appear in: *European Journal of Medicinal Chemistry*

Received Date: 25 October 2017

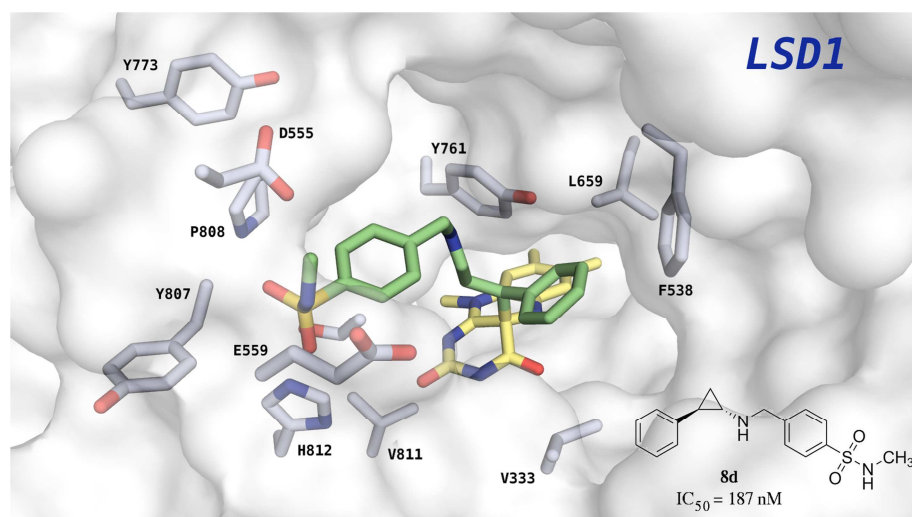
Revised Date: 28 November 2017

Accepted Date: 1 December 2017

Please cite this article as: J. Schulz-Fincke, M. Hau, J. Barth, D. Robaa, D. Willmann, A. Kürner, J. Haas, G. Greve, T. Haydn, S. Fulda, M. Lübbert, S. Lüdeke, T. Berg, W. Sippl, R. Schüle, M. Jung, Structure-activity studies on *N*-Substituted tranlycypromine derivatives lead to selective inhibitors of lysine specific demethylase 1 (LSD1) and potent inducers of leukemic cell differentiation, *European Journal of Medicinal Chemistry* (2018), doi: 10.1016/j.ejmech.2017.12.001.

This is a PDF file of an unedited manuscript that has been accepted for publication. As a service to our customers we are providing this early version of the manuscript. The manuscript will undergo copyediting, typesetting, and review of the resulting proof before it is published in its final form. Please note that during the production process errors may be discovered which could affect the content, and all legal disclaimers that apply to the journal pertain.





Structure-Activity Studies on *N*-Substituted  
Tranylcypromine Derivatives Lead to Selective  
Inhibitors of Lysine Specific Demethylase 1 (LSD1)  
and Potent Inducers of Leukemic Cell  
Differentiation

*Johannes Schulz-Fincke*<sup>†, ‡, §</sup>, *Mirjam Hau*<sup>†</sup>, *Jessica Barth*<sup>†, ‡</sup>, *Dina Robaa*<sup>||</sup>, *Dominica Willmann*<sup>⊥</sup>,  
*Andreas Kürner*<sup>†, ‡, §</sup>, *Julian Haas*<sup>†</sup>, *Gabriele Greve*<sup>⊥, #</sup>, *Tinka Haydn*<sup>‡, †, §</sup>, *Simone Fulda*<sup>‡, †, §</sup>,  
*Michael Lübber*<sup>⊥, ‡</sup>, *Steffen Lüdeke*<sup>†</sup>, *Tobias Berg*<sup>†, ‡</sup>, *Wolfgang Sippl*<sup>||</sup>, *Roland Schüle*<sup>⊥</sup>, and  
*Manfred Jung*<sup>†\*</sup>

<sup>†</sup> Institute of Pharmaceutical Sciences, University of Freiburg (Germany)

<sup>‡</sup> German Cancer Consortium (DKTK), Freiburg (Germany)

<sup>§</sup> German Cancer Research Center (DKFZ), Heidelberg (Germany)

<sup>||</sup> Institute of Pharmacy, Martin-Luther-University of Halle-Wittenberg (Germany)

⊥ Department of Urology/Women's Hospital and Center for Clinical Research, University of Freiburg Medical Center (Germany)

⊞ German Cancer Consortium (DKTK), Frankfurt (Germany)

⊚ Division of Hematology, Oncology and Stem Cell Transplantation, Department of Internal Medicine, University of Freiburg Medical Center (Germany)

# Faculty of Biology, University of Freiburg (Germany)

⋮ Institute for Experimental Cancer Research in Pediatrics, Goethe-University Frankfurt (Germany)

**KEYWORDS:** Epigenetics, KDM1A, AML, small molecule inhibitors, SAR, mechanism-based inhibitors

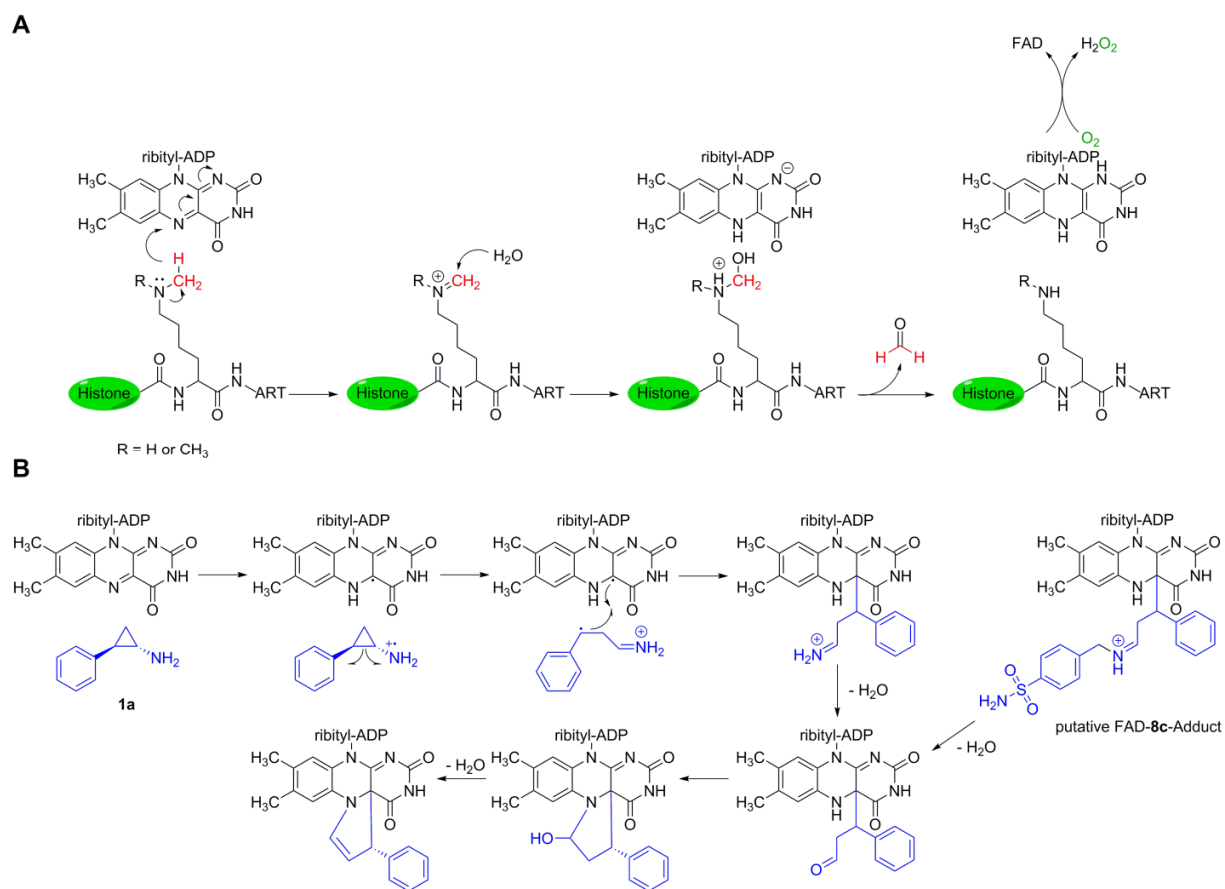
**Abbreviations:** AML, acute myeloid leukemia; MAOs, Monoamine oxidases A and B; HRP, Horseradish peroxidase; TLC, thin layer chromatography; vdW, van-der-Waals; CFU Colony forming units; Copper(II) acetylacetonate, Cu(acac)<sub>2</sub>; Ethyl diazoacetate, EDA; DFT, density functional theory.

## ABSTRACT

FAD-dependent lysine-specific demethylase 1 (LSD1) is overexpressed or deregulated in many cancers such as AML and prostate cancer and hence is a promising anticancer target with first inhibitors in clinical trials. Clinical candidates are *N*-substituted derivatives of the dual LSD1-/monoamine oxidase-inhibitor tranylcypromine (2-PCPA) with a basic amine function in the *N*-substituent. These derivatives are selective over monoamine oxidases. So far, only very limited information on structure-activity studies about this important class of LSD1 inhibitors is published in peer reviewed journals. Here, we show that *N*-substituted 2-PCPA derivatives without a basic function or even a polar group are still potent inhibitors of LSD1 *in vitro* and effectively inhibit colony formation of leukemic cells in culture. Yet, these lipophilic inhibitors also block the structurally related monoamine oxidases (MAO-A and MAO-B) which may be of interest for the treatment of neurodegenerative disorders, but this property is undesired for applications in cancer treatment. The introduction of a polar, non-basic function led to optimized structures that retain potent LSD1 inhibitors but exhibit selectivity over MAOs and are highly potent in the suppression of colony formation of cultured leukemic cells. Cellular target engagement is shown via a Cellular Thermal Shift Assay (CETSA) for LSD1.

## Introduction

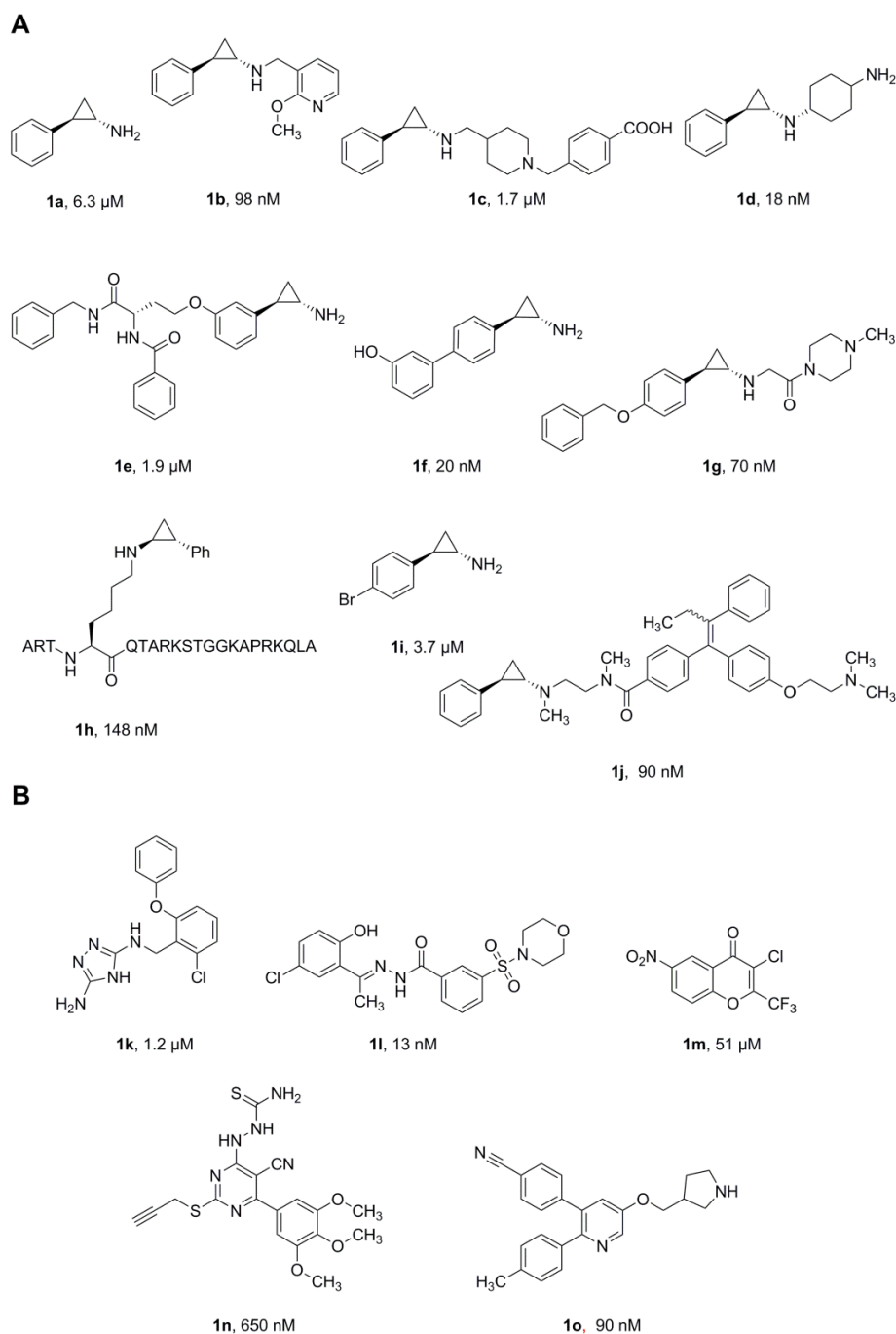
LSD1 (KDM1A) is an epigenetic modifier that demethylates distinct mono- and dimethylated lysines in histones, but also non-histone proteins, such as p53 *via* a FAD-dependent mechanism. Methylation at H3K4 is generally associated with gene activation, as removal of this mark by LSD1 leads to transcriptional repression. Upon interaction with the androgen receptor, LSD1 shifts the demethylation to H3K9me and promotes gene activation.[1] In the monoamine oxidase reaction, FAD is reduced to FADH<sub>2</sub> with concomitant conversion of the substrates *N*-methyl group to an imine intermediate. This is hydrolyzed subsequently and decomposes to formaldehyde and the demethylated lysine. Simultaneously the cofactor is reoxidized by consuming molecular oxygen which forms hydrogen peroxide (Scheme 1 A).[2] During the last decade, LSD1 has emerged as a key epigenetic regulator of various disease states and hence represents a promising drug target. It regulates cellular signaling pathways in various cancer entities such as breast cancer where it interacts in a deacetylase containing multiprotein complex (NuRD).[3] In prostate cancer high levels of LSD1 are associated with cancer progression and metastasis and hence LSD1 levels could be a useful biomarker.[4, 5] Harris *et al* described the consequence of overexpression of LSD1 in MLL-AF9 leukemia stem cells and the use of potent LSD1 inhibitors (**1b**) to induce the differentiation and decrease of the clonogenic potential. Similar effects have been described for other hematopoietic lineages as well, when LSD1 was inhibited by small molecules or a knockdown was performed using siRNA. Hematopoiesis is regulated by the genes *Hoxa9*, *Meis1* and *Gfi1b* among others, which are critically up-regulated by LSD1.[6, 7] The enzyme's activity affects key cellular events, like gene expression, metabolic processes and maintenance of oncogenes. Besides cancer, LSD1 has also been proposed as a target for the treatment of neuronal diseases.[8-11]

**Scheme 1.** Catalytic mechanism of LSD1 and activation of 2-PCPA.

**(A)** Catalytic mechanism of KDM1A; **(B)** Activation of 2-PCPA and formation of FAD-adduct. The putative FAD-8c-adduct is shown according to the known mechanism.

Due to the great therapeutic potential of LSD1 inhibition, quite a large number of inhibitors has been described and the first two selective inhibitors (**1c**,**1d**)[12, 13] have already advanced to clinical trials for the treatment of cancer and neurodegenerative diseases.[14, 15] The prototypical LSD1 inhibitor is *trans*-2-PCPA (**1a**) which was approved for the treatment of depression based on its covalent inhibition of MAOs. *trans*-2-PCPA is also in clinical trials for AML treatment but derivatives show significantly increased potency and compounds with significant selectivity over MAOs have been identified. Generally, LSD1 inhibitors can be

distinguished between reversible and irreversible inhibitors of LSD1. The irreversible inhibitors **1a-1j**[11, 16-20] (Figure 1 A) are suicide inhibitors. Protein crystallography shows evidence for the formation of a covalent adduct with the cofactor after an FAD-dependent activation process (Scheme 1 B). Upon activation, the cyclopropyl structure undergoes a ring opening and subsequently forms a new bond with the cofactor at position N(5) and C(4a). Crystal structures of FAD adducts with either (1*R*,2*S*) or (1*S*,2*R*) *trans*-2-PCPA, respectively, show that its orientation depends on the absolute configuration of the inhibitor.[16, 21, 22] Examples for reversible compounds **1k-1o**[1, 23-26] are mentioned in Figure 1B.



Substitution with hydrophobic groups in the cyclopropyl ring of 2-PCPA at 1-position such as alkyl and aryls increase the activity against LSD1, whereas esters and carboxylic acids in this position decrease the inhibitory effect.[27, 28] To increase the potency and selectivity of 2-PCPA, modifications both on the phenyl ring and the nitrogen have been performed (**1e-g**, **1i**). Detailed structure-activity studies are available for phenyl-ring substituted compounds. Derivatization in *meta* and *para* position of the phenyl ring leads to IC<sub>50</sub> values in lower nanomolar range and potent cellular activity.[29, 30] There are patents and publications on studies employing *N*-alkylated analogues as selective LSD1 inhibitors but the SAR is not discussed profoundly and mostly a few potent derivatives are presented with emphasis on biological effects.[31-33] Hence, we wanted to investigate the effect of *N*-substitution on biological activity.

In the present study, we investigate the SAR of *N*-alkylated derivatives of the parent *trans*-2-PCPA (**1a**, Figure 1) which is not well documented in the scientific literature. Firstly, we present the introduction of a methyl group in the unsubstituted position of the cyclopropyl ring leading to series **6** (Table 1). Subsequently, *N*-alkylation is the major focus of this study and resulted in a series of highly potent LSD1 inhibitors, that have a disubstituted cyclopropane ring (series **7** and **8**, Table 2 and 3), with IC<sub>50</sub> values in the lower nanomolar range. We provide an insight in how substitutions have an effect on selectivity and show that selected compounds exhibit strong antileukemic properties in different cellular models.

## Results and discussion.

Based on the mechanism of *trans*-2-PCPA activation, we reasoned that a methyl group at the usually unsubstituted position of the cyclopropyl ring might stabilize the formed radical in alpha position to the carbon which is substituted by the methyl group and could result in inhibitors with superior potency compared to *trans*-2-PCPA or *N*-substituted derivatives without a methyl group at this position.

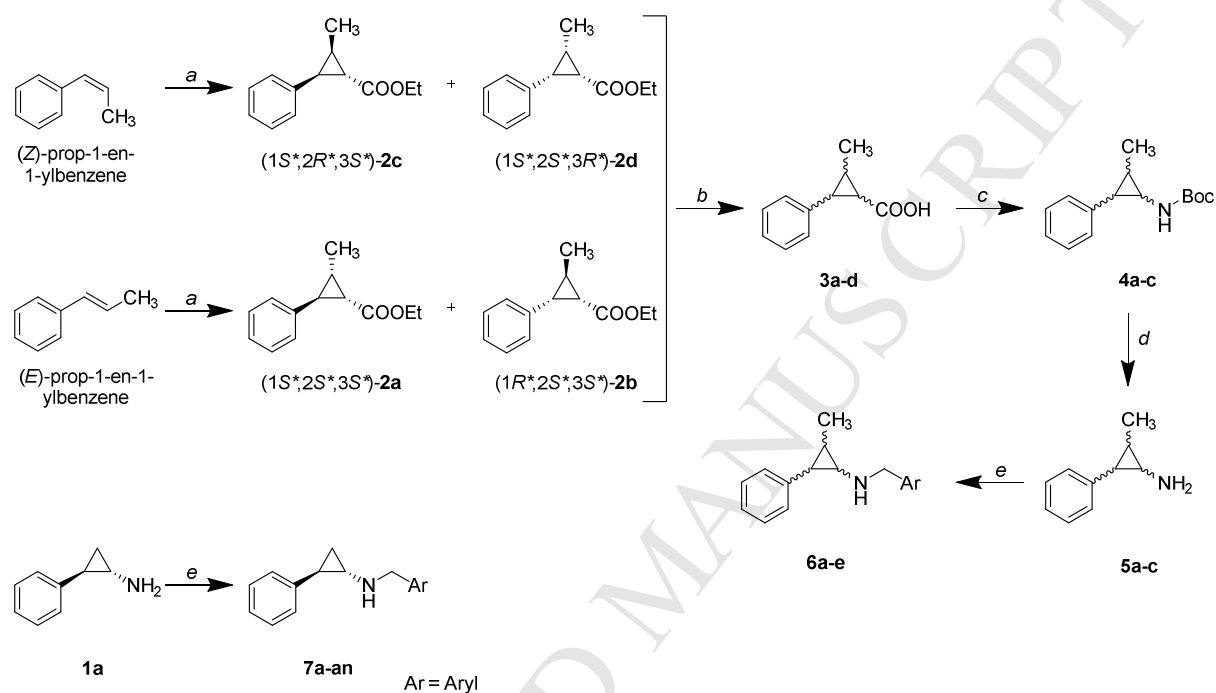
For the synthesis of the cyclopropyl ring a copper-catalyzed cyclopropanation was used. The stereochemistry of the reaction leads preferably to *trans*-oriented substituents at the cyclopropyl ring.[34] In addition to the *trans*-selective cyclopropanation, the relative orientation of the third substituent is controlled by the stereochemistry of the starting olefin (Scheme 2). *Z*-methyl styrene leads to a *cis*-oriented phenyl and methyl group and accordingly, the *E*-congener places the phenyl and the methyl group on different sides of the cyclopropane plane. We used copper(II) acetylacetonate as a catalyst precursor instead of the catalytically active species Cu(I) due to stability reasons. A wide range of metal catalysts such as Rh, Ru and Co are suitable to initiate the intramolecular cyclopropanation through decomposition of the  $\alpha$ -diazoester.[35] With a good yield of 60-70 % in total we stopped the reaction after 4 hours and separated the *cis* and *trans* isomers ethyl (1*S*\*,2*S*\*,3*S*\*)-2-methyl-3-phenylcyclopropane-1-carboxylate (**2a**) and the (1*R*\*,2*S*\*,3*S*\*)-diastereomer (**2b**) by flash chromatography (see Scheme 2). The appropriate styrene could be recycled and reused in further batches. We analyzed **2a** and **2b** by NMR to determine the relative configuration (Figure S1).

Due to the nature of the cyclopropanation the relative orientation of the phenyl and the methyl group is *trans*. We observed an H-H-coupling with  $J_{cis} = 9.3$  Hz for the protons next to the ester and the methyl group in **2a**, implying that ester and phenyl group are both *trans*-oriented as well.

The same coupling constant ( $J_{cis} = 9.3$  Hz) has been noticed for the protons next to the ester and phenyl moiety in **2b**. These coupling constants of **2a** and **2b** corresponds to literature values.[36] Upon mild hydrolysis in methanol, the corresponding carboxylic acids (**3a** and **3b**) were heated with diphenylphosphoryl azide and triethylamine in toluene to form a cyclopropyl carbonyl azide which decomposes in a Curtius rearrangement when heated in solvent to 120 °C. This leads to a cyclopropyl isocyanate which reacts with added anhydrous *tert*-ButOH to a Boc protected amine (**4a**, **4b**) in 50-70 % yield. Free unprotected amine is scavenged by di-*tert*-butyldicarbonate. The mixture of **2c** and **2d** could not be separated as esters and carboxylic acids (**3c** and **3d**) and was used as a mixture for the Curtius rearrangement to get **4c** in low yields but not its diastereomer. Removal of the Boc protecting group using 2 M HCl in 1,4-dioxane afforded cyclopropylamines **5a-c** as hydrochlorides. The relative configuration of **5c** was determined via NMR with a coupling of  $J_{cis} = 8.7$  Hz for protons 1 and 3 and thus resulting in the structure of **5c** and its precursors, as depicted in Table 1.

As it had been shown that *trans*-2-PCPA was more potent than the *cis*-isomer, we only synthesized the *trans*-oriented target compounds.[22] *N*-alkylation was achieved by reductive amination of the primary amine using aldehydes and sodium triacetoxyborohydride as the reducing agents to yield the compounds in Table 1 and 2.

**Scheme 2.** General route of the synthesis for di- and trisubstituted substrates. All compounds were produced as racemates and the depicted stereochemistry reflects the relative orientation of the groups, i.e. only one enantiomer is displayed.

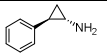
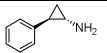
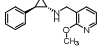
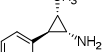
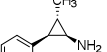
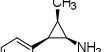
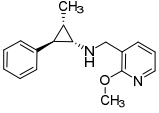
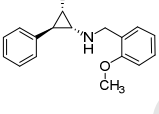
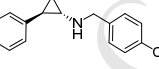
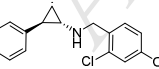
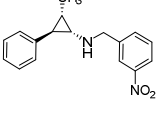


Reagents and conditions: (a)  $\text{Cu}(\text{acac})_2$ , EDA, DCM, 60 °C, 4 h; (b) KOH, MeOH, over night; (c)  $\text{NEt}_3$ , DPPA,  $\text{Boc}_2\text{O}$ , *tert*-butanol, 120 °C, 12 h; (d) 1,4-dioxane, 2 M HCl, over night; (e) STAB, appropriate aldehyde, DCE, 2h.

For *in vitro* testing the standard Peroxidase assay was used employing a truncated dimethyl histone peptide ( $\text{H3K4}_{\text{aa1-20}}$ ) as substrate and quantification of the product hydrogen peroxide using 10-acetyl-3,7-dihydroxyphenoxazine. Unexpectedly, all trisubstituted cyclopropanes were devoid of LSD1 inhibitory activity, even in the presence of *N*-substituents that lead to highly potent analogues when appended to tranylcypromine. C-methylation completely abolished LSD1 inhibitory activity (e.g. **7v** vs. **6c**). The assay kit MAO-Glo was used for selectivity determination against MAOs. Some of these derivatives were fairly potent inhibitors of

monoamine oxidase A with  $IC_{50}$  values in the nanomolar range and showed moderate activity against monoamine oxidase B (Table 1) and they could be used as negative controls for target engagement and assay development with 2-PCPA based LSD1 inhibitors in biological studies.

**Table 1.** Inhibition values of trisubstituted 2-PCPA analogues.

Compound		$IC_{50}$ [nM] or inhibition [%]		
		LSD1	MAO-A	MAO-B
<b>1a</b>		$6.5 \cdot 10^3$	$3.4 \cdot 10^3$	-
<b>1b</b>		$65.5 \pm 3.5$	n.i. <sup>b</sup>	n.i. <sup>b</sup>
<b>5a</b>		n.i. <sup>a</sup>	n.i. <sup>b</sup>	n.i. <sup>b</sup>
<b>5b</b>		n.i. <sup>a</sup>	n.i. <sup>b</sup>	n.i. <sup>b</sup>
<b>5c</b>		n.i. <sup>a</sup>	n.i. <sup>b</sup>	n.i. <sup>b</sup>
<b>6a</b>		n.i. <sup>c</sup>	$41.4 \cdot 10^3$	14% <sup>b</sup>
<b>6b</b>		n.i. <sup>c</sup>	32% <sup>b</sup>	n.i. <sup>b</sup>
<b>6c</b>		n.i. <sup>b</sup>	$310 \pm 66$	$10.5 \cdot 10^3$
<b>6d</b>		n.i. <sup>a</sup>	$780 \pm 140$	$56.2 \cdot 10^3$
<b>6e</b>		n.i. <sup>b</sup>	$237 \pm 45$	$2.2 \cdot 10^3$

IC<sub>50</sub> values were calculated from at least 8 data points and are the mean of at least two independent determinations; (a) Percentage of inhibition at 100 μM; (b) Percentage of inhibition at 10 μM; (c) unspecific, not dose-dependent low inhibition; (n.i.) no inhibition

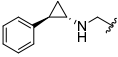
As the sterical demand of the 3-methyl group seems to prevent LSD1 binding, we focused subsequently on *N*-alkylation to achieve higher potency and selectivity against LSD1. There is little precedence in peer reviewed journals on structure-activity studies of *N*-alkylation despite a wealth of patent examples. To get an overview of the effect of non-basic compounds, we synthesized some of the examples mentioned in the referred patents.[37] Based on the structure of compounds used in clinical trials (**1c**, **1d**) and on analyses in a series of reversible inhibitors that are thought to have overlapping binding sites with the *N*-substituted derivatives, it was postulated that a basic moiety (aliphatic amine or pyridine) in the substituent is required for LSD1 inhibitors that are both potent and selective (e.g. **1b** and **1d**).[38]

To actually probe this hypothesis, we prepared a series of *N*-substituted tranylcyromines that mostly bear lipophilic or weakly polar substituents, such as **7b** or **7ad**. *N*-substitution was again achieved by reductive animation of *trans*-2-PCPA. We were pleased to see that potent LSD1 inhibitors can be identified among lipophilic *N*-substituted tranylcyromines.

In this series we synthesized single and multiple halide substitutions at different positions which led to potent compounds in all cases without selectivity over MAOs, though. The similar IC<sub>50</sub> values support our conclusion that LSD1 does not have a general preference for *ortho*-*meta*- or *para*- halide resp. methoxy-substituted compounds (Table 2). Those non-pyridine analogues of **1b** showed good potency but less selectivity regarding MAOs. An exception is the nitro substitution as the IC<sub>50</sub> of the *ortho*-substituted phenyl group in compound **7ac** is 6-fold higher than the one of its *meta*-isomer **7ad**. We observed selectivity over MAOs by using the pyridine moiety in **7b**, which already improves the potency compared to *trans*-2-PCPA. The

combination of methoxy group and pyridine had been published as a very potent and selective compound (**1b**). With our methodology we determined an  $IC_{50}$  of  $65.5 \pm 3.5$  nM for reference inhibitor **1b** (literature value 98 nM).

ACCEPTED MANUSCRIPT

**Table 2.** IC<sub>50</sub> values of 2-PCPA derivatives with nonpolar substituents


Compound	IC <sub>50</sub> [nM]			Compound	IC <sub>50</sub> [nM]				
	LSD1	MAO-A	MAO-B		LSD1	MAO-A	MAO-B		
<b>7a</b>		321.1 ± 69.7	5.7 · 10 <sup>3</sup>	33% <sup>a</sup>	<b>7u</b>		103.9 ± 3.1	62% <sup>a</sup>	21% <sup>a</sup>
<b>7b</b>		202.4 ± 4.4	n.i. <sup>a</sup>	n.i. <sup>a</sup>	<b>7v</b>		77.5 ± 16.3	205.5 ± 13.4	14.1 · 10 <sup>3</sup>
<b>7c</b>		66.1 ± 0.1	9.7 · 10 <sup>3</sup>	36% <sup>a</sup>	<b>(S,R)-7v</b>		95.6 ± 4.8	-	-
<b>7d</b>		157.9 ± 5.5	79% <sup>a</sup>	n.i. <sup>a</sup>	<b>(R,S)-7v</b>		94.9 ± 16.3	-	-
<b>7e</b>		100.2 ± 27.2	30% <sup>b</sup>	n.i. <sup>b</sup>	<b>7w</b>		202.8 ± 41.9	73% <sup>a</sup>	11% <sup>a</sup>
<b>7f</b>		110.0 ± 2.4	69% <sup>a</sup>	n.i. <sup>a</sup>	<b>7x</b>		122.0 ± 12.2	30% <sup>b</sup>	17% <sup>b</sup>
<b>7g</b>		95.9 ± 8.2	47% <sup>a</sup>	24% <sup>a</sup>	<b>7y</b>		64.5 ± 36.6	69% <sup>b</sup>	n.i. <sup>b</sup>
<b>7h</b>		112.1 ± 14.2	38% <sup>b</sup>	n.i. <sup>b</sup>	<b>7z</b>		276.5 ± 12.0	33% <sup>b</sup>	12% <sup>b</sup>
<b>7i</b>		294.5 ± 30.1	43% <sup>a</sup>	27% <sup>a</sup>	<b>7aa</b>		817.1 ± 19.0	22% <sup>b</sup>	27% <sup>b</sup>
<b>7j</b>		79.7 ± 18.3	27% <sup>b</sup>	n.i. <sup>b</sup>	<b>7ab</b>		91.1 ± 20.4	12% <sup>b</sup>	16% <sup>b</sup>
<b>7k</b>		117.5 ± 2.1	20% <sup>a</sup>	16% <sup>a</sup>	<b>7ac</b>		643.5 ± 14.9	18% <sup>b</sup>	15% <sup>b</sup>
<b>7l</b>		108.5 ± 2.1	69% <sup>a</sup>	20% <sup>a</sup>	<b>7ad</b>		99.5 ± 6.4	488.5 ± 36.1	1.4 · 10 <sup>3</sup>
<b>7m</b>		114.1 ± 28.6	27% <sup>b</sup>	n.i. <sup>b</sup>	<b>(S,R)-7ad</b>		51.8 ± 8.8	-	-
<b>7n</b>		100.0 ± 18.4	43% <sup>b</sup>	n.i. <sup>b</sup>	<b>(R,S)-7ad</b>		111.7 ± 2.4	-	-
<b>7o</b>		159.0 ± 42.4	27% <sup>b</sup>	n.i. <sup>b</sup>	<b>7ae</b>		35.3 ± 3.5	100% <sup>a</sup>	13% <sup>a</sup>
<b>7p</b>		117 ± 0.1	94% <sup>b</sup>	79% <sup>b</sup>	<b>7af</b>		154.5 ± 9.2	93% <sup>b</sup>	52% <sup>b</sup>
<b>7q</b>		119.9 ± 28.6	93% <sup>b</sup>	82% <sup>b</sup>	<b>7ag</b>		82.6 ± 5.0	100% <sup>b</sup>	44% <sup>b</sup>
<b>7r</b>		60.0 ± 4.2	160.5 ± 23.33	n.i. <sup>a</sup>	<b>7ah</b>		66.5 ± 0.3	60% <sup>b</sup>	23% <sup>b</sup>
<b>7s</b>		325 ± 34.8	48% <sup>a</sup>	17% <sup>a</sup>	<b>7ai</b>		80.7 ± 2.7	100% <sup>b</sup>	32% <sup>b</sup>
<b>7t</b>		417.5 ± 3.5	30% <sup>b</sup>	n.i. <sup>b</sup>	<b>7aj</b>		69.1 ± 1.0	54% <sup>a</sup>	14% <sup>a</sup>

The IC<sub>50</sub> values were calculated from at least 8 data points and are the mean value of at least two independent determinations; (n.i.) no inhibition; (-) not determined; (a) Percentage of inhibition at 10 μM; (b) Percentage of inhibition at 1 μM. All compounds are racemates and only one enantiomer (relative configuration) is depicted (unless marked otherwise).

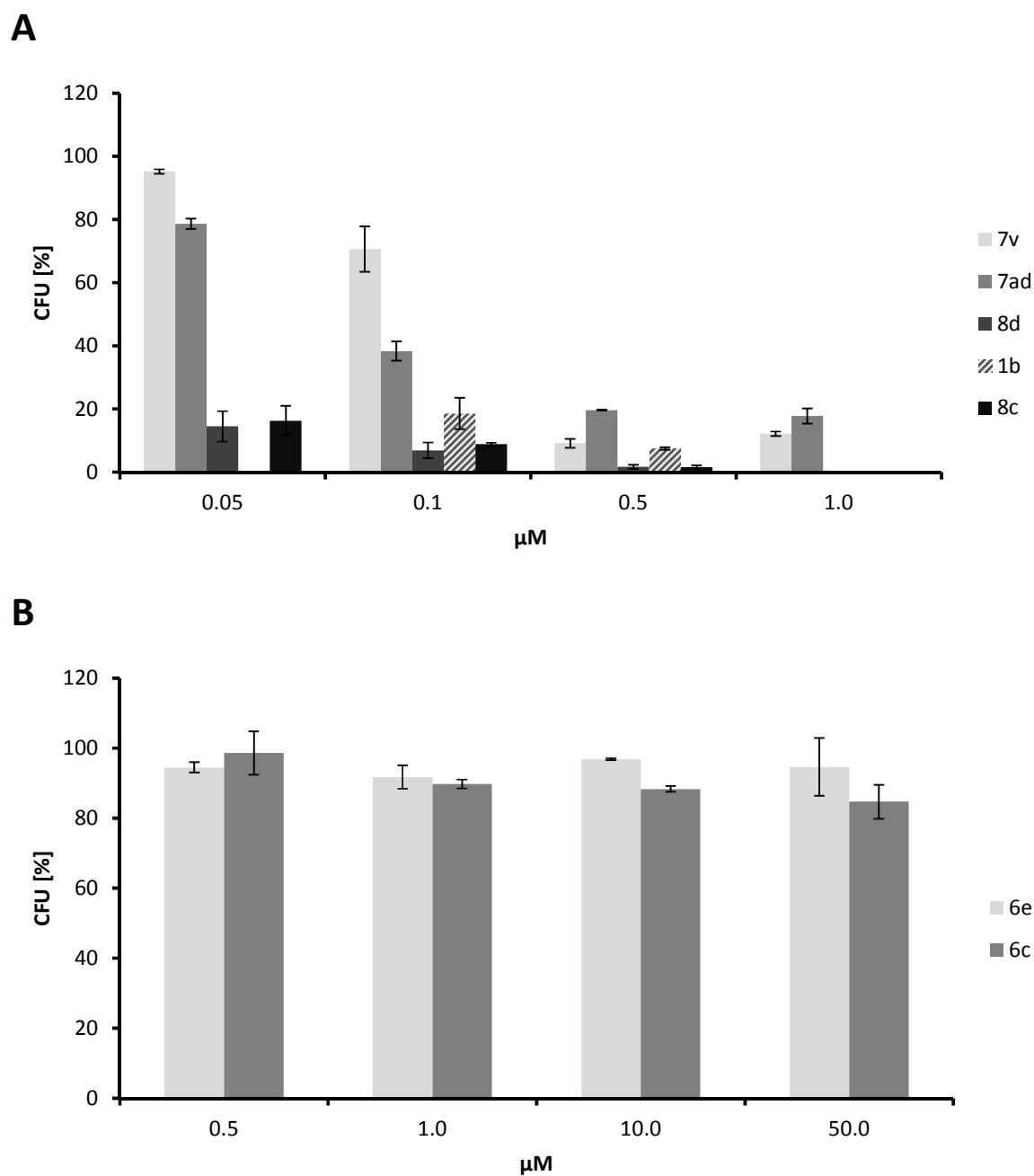
The inhibitor potency is significantly decreased by alkyl substituents, at least in *para* position of the *N*-benzyl moiety (**7z**, **7aa**). To elucidate how far the compounds can be extended in size, we synthesized derivatives with larger and bulkier *N*-substituents, again with and without a halide substitution. Both biphenyl analogues exhibit a nanomolar effect *in vitro*, but the *meta*-substituted derivative has a twofold lower IC<sub>50</sub> against LSD1. This was also observed for benzyloxybenzyl analogues where the *meta*-isomer **7ah** shows also a twofold higher affinity than its *para* analogue **7af**. Interestingly, a bromo substitution increased the potency in the *para* aryloxy compound **7ag** to the level of the *meta*-congener **7ai**.

Furthermore, we wanted to clarify the contribution of the stereochemistry for the *in vitro* potency. It has already been shown that the enantiomers of *trans*-2-PCPA slightly differ in their IC<sub>50</sub> values.[22] To elucidate whether this effect has also been amplified by activity enhancement from *N*-alkylation, we investigated the biological activity of the single enantiomers of **7v** and **7ad**. We separated the stereoisomers by the use of chiral HPLC on a semipreparative scale. Indeed, the biological evaluation revealed that (1*S*,2*R*)-**7ad** is more potent than (1*R*,2*S*)-**7ad** while the IC<sub>50</sub> values for the two enantiomers (1*S*,2*R*)-**7v** and (1*R*,2*S*)-**7v** are similar to the IC<sub>50</sub> value of racemic **7v**. The absolute configuration of (1*S*,2*R*)-**7ad** and (1*R*,2*S*)-**7ad** were assigned by comparison of vibrational circular dichroism (VCD) spectra to spectra from quantum chemical calculations – a well-established method for the determination of the absolute configuration (Figure S2).[39] Different from electronic CD, which samples electronic transitions in chiral molecules, VCD provides characteristic spectral patterns from 6N–3

vibrational modes and does not depend on the existence of a chromophoric system. The high content of structural information in these spectral patterns and the comparable high accuracy of spectrum prediction (usually on DFT level) makes VCD a highly valuable tool for the stereochemical analysis and is nowadays widely applied for drug molecules.[40]

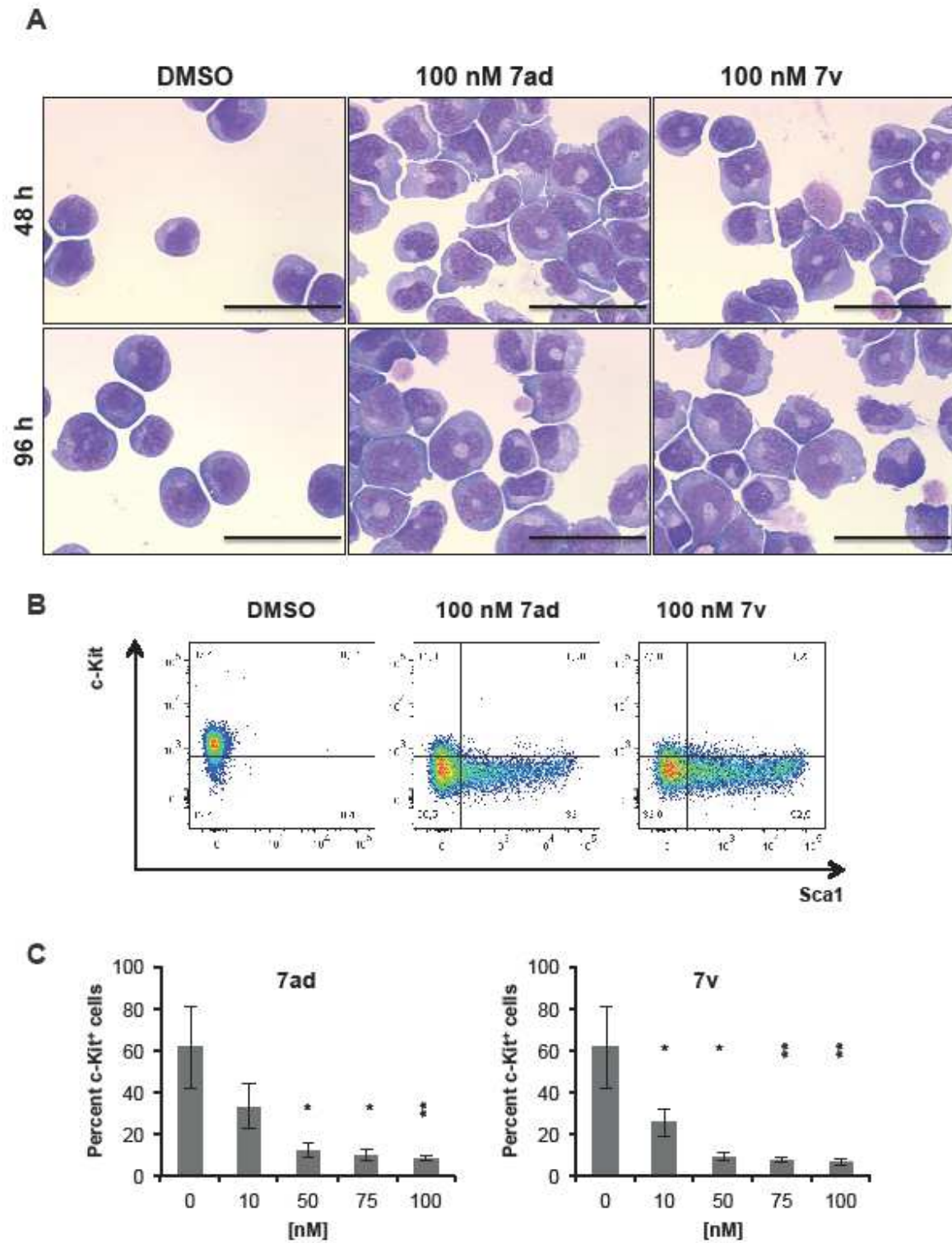
**7v** and **7ad** were also rather potent inhibitors of MAO-A but not MAO-B. Thus, while *N*-benzylation is sufficient to increase LSD1 inhibitory potency substantially, it does not lead to selectivity over MAOs. We still investigated the activity of compounds in cellular models that have previously been shown to respond strongly to LSD1 inhibition. The colony-forming unit assay (CFU assay) is enumerating hematopoietic progenitor cancer cells with colony formation potential. Treatment with LSD inhibitors decreases the number of units and allows the quantification of the effect of inhibitors on cancer entities.

First, we tested the unselective compounds **7v** and **7ad** for their antileukemic properties. They showed an effect when THP1 cells were treated with nanomolar concentrations and decreased the number of colony forming units by 80 % at 0.5  $\mu$ M (Figure 2 A). In contrast the trisubstituted analogues **6c** and **6e** did not show any influence in this cell line even at higher concentrations, which is in accordance with an inactivity toward LSD1 (Figure 2 B). However, the reduction of colony formation is not specific for only LSD1 inhibition which is why we showed target engagement of LSD1 with the compounds **7v** and **7ad** in the CETSA (Fig. 6) in the same cell line as was used in the colony forming unit assay.



**Figure 2.** Antileukemic effect on THP-1 cells of selected compounds; (A) *N*-benzylated compounds reduce ability to create colony forming units, **1b** is used as reference inhibitor at the concentration of 0.1 and 0.5 μM; (B) no cellular effect of trisubstituted 2-PCPA analogues even at high concentrations.

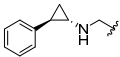
It has previously been shown that LSD1 inhibition induces differentiation in murine and mammalian leukemia models[6, 41, 42]. In order to evaluate the differentiation effects induced by LSD1 inhibition *in vitro*, we used Hoxa9/Meis1-transformed murine progenitor cells that elicit leukemia upon injection into irradiated recipient mice. Cells were treated with increasing concentrations of **7v** and **7ad** and analyzed for morphological signs of granulocytic differentiation as well as changes in surface marker expression. We observed differentiation including characteristic changes in nuclear morphology (Figure 3 A). It is known that the leukemic stem cell population in murine leukemia models resides in the c-Kit-positive fraction.[43] We therefore used flow cytometric analysis to determine the reduction in the fraction of c-Kit-positive cells upon treatment with the LSD1 inhibitors **7v** and **7ad** (Figure 3 B). Both compounds induced differentiation effects even at 50 nM and led to a reduction in c-Kit-positive cells suggesting a good cellular penetration and potency (Figure 3 C).



**Figure 3.** Inhibition of LSD1 by **7v** and **7ad** induces granulocytic differentiation and loss of c-Kit-expressing immature cells in Hoxa9/Meis1-transformed hematopoietic progenitors. **(A)** Representative images of cyospin preparations of Hoxa9/Meis1 cells after treatment with 100 nM of **7v** or **7ad** at indicated time points stained with Pappenheim stain, Scale bar: 50  $\mu$ m; **(B)** Representative flow cytometric analysis for c-Kit and Sca1 in Hoxa9/Meis1-transformed myeloid progenitors; **(C)** Quantitative analysis of c-Kit-positive cells in Hoxa9/Meis1-transformed cells as analyzed by flow cytometry. Cells were treated with indicated concentrations of LSD1 inhibitors **7v** and **7ad** for 96 h. The mean percentage  $\pm$  SEM of c-Kit-positive cells from 3 experiments is shown; \*  $p \leq 0.05$ , \*\*  $p \leq 0.01$

Given that strongly basic tertiary amines as well as the weakly basic pyridine in inhibitor **1b** give rise to compounds that are potent and selective, we reasoned that just a polar function might be enough to increase selectivity over monoamine oxidases. Hence, we prepared a second series of *N*-benzylated tranylcypromines with more polar substituents. For example the sulfonamide **8c** and the *N*-methylsulfonamide **8d** have calculated logP-values of 1.0 resp. 2.0 as opposed to 2.5 in derivative **7v** (predicted with *Schrödinger* suite 2013).[44]

The compounds **8a-e** retained the strong inhibitory properties of the lipophilic series on LSD1 with  $IC_{50}$  values below 200 nM (Table 3). As already observed in the first series, the *meta*-substituted compound is again more potent than *ortho* substituted derivatives. Different from the first series, they also present significant selectivity over MAOs with compound **8c** showing the best selectivity. The compounds **8c** and **8d** also showed even more potent antileukemic properties and reduced the count of CFUs by 80 % at only 50 nM (Figure 2 A).

**Table 3.** IC<sub>50</sub> values of tranylcypromine derivatives with polar substituents


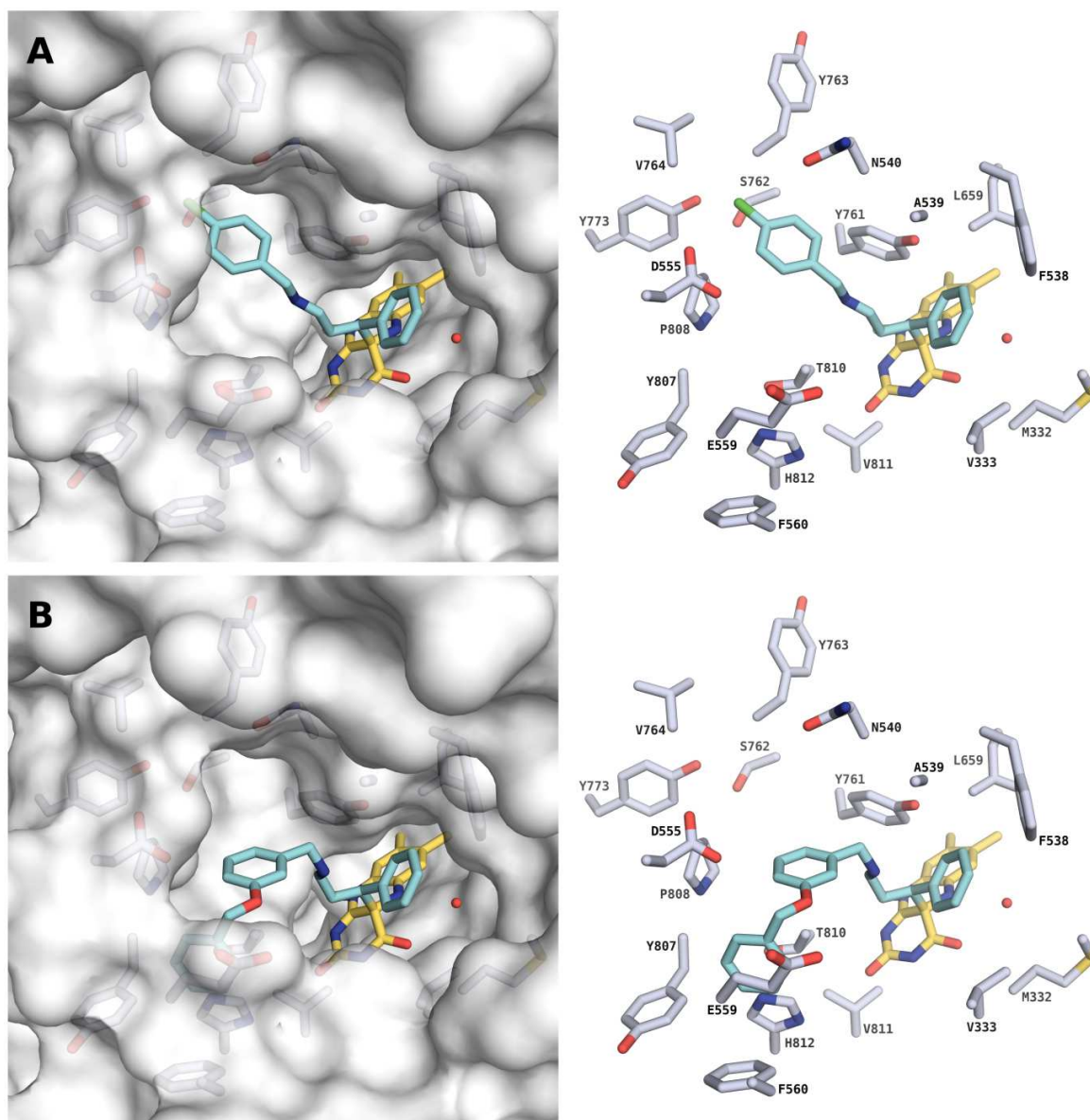
Compound	IC <sub>50</sub> [nM]			Selectivity	
	LSD1	MAO-A	MAO-B	MAO-A/LSD1	MAO-B/LSD1
<b>8a</b> 	91.0 ± 0.2	27.9 · 10 <sup>3</sup>	95.7 · 10 <sup>3</sup>	307	1052
<b>8b</b> 	194.6 ± 7.4	24.7 · 10 <sup>3</sup>	50% <sup>a</sup>	127	>1282
<b>8c</b> 	146.5 ± 0.1	21.6 · 10 <sup>3</sup>	42% <sup>a</sup>	147	>1700
<b>8d</b> 	187.3 ± 0.1	17.1 · 10 <sup>3</sup>	n.i. <sup>a</sup>	91	>1337

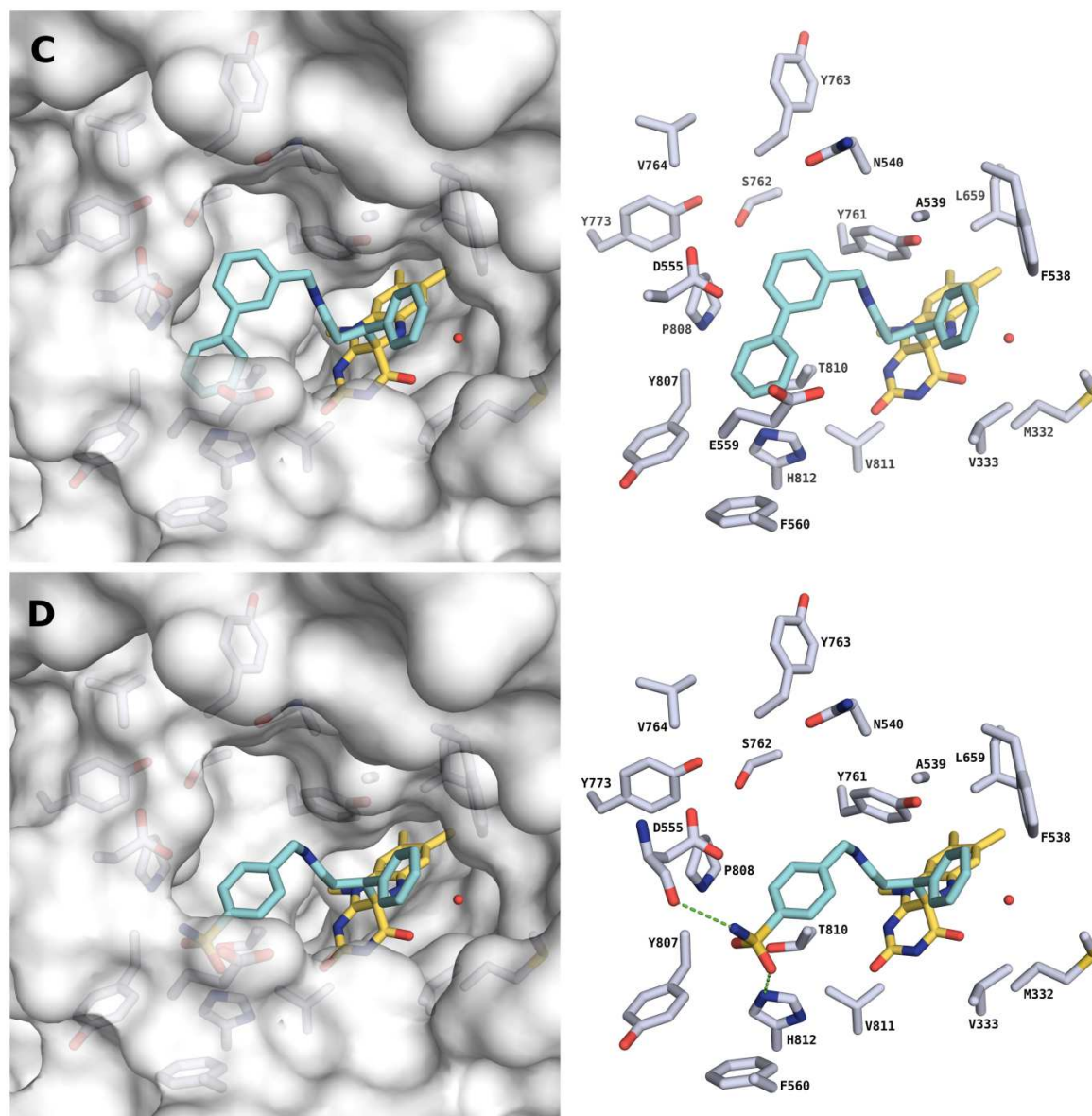
The IC<sub>50</sub> values were calculated from at least 8 data points and are the mean value of at least two independent determinations; (n.i.) no inhibition; (a) Percentage of inhibition at 250 μM; All compounds are racemates and only one enantiomer is depicted.

To rationalize the observed selectivity profiles of the herein described *N*-substituted 2-PCPA derivatives and to predict the interaction for LSD1, molecular docking was performed. As already mentioned 2-PCPA derivatives bearing polar substituents at the *N*-benzyl group (**8c** and **8d**) show a preference for LSD1 over MAOs. Meanwhile, 3-methyl-2-PCPA derivatives completely lack activity for LSD1, however, some still display considerable activity for MAO-A. Previous studies as well as crystal structure analysis of LSD1-2-PCPA derivatives[21, 22, 28, 45] demonstrate the formation of either N5, C4a or cyclic adducts with the cofactor FAD. In the case of MAO-B, available crystal structures reveal the formation of the C4a-adduct.[46] Based on the co-crystallized ligand structure of the C4a-adduct of the 1-ethyl-2-PCPA derivative in complex with LSD1[28] and of 2-PCPA with MAO-B[46], similar C4a adducts of the herein reported compounds were modelled as *N*-benzyl-imines and subsequently docked into the crystal

structures of LSD1 (PDB ID 4UV8)[28] and MAO-A (PDB ID 2BXS)[47] using the program Glide.[48]

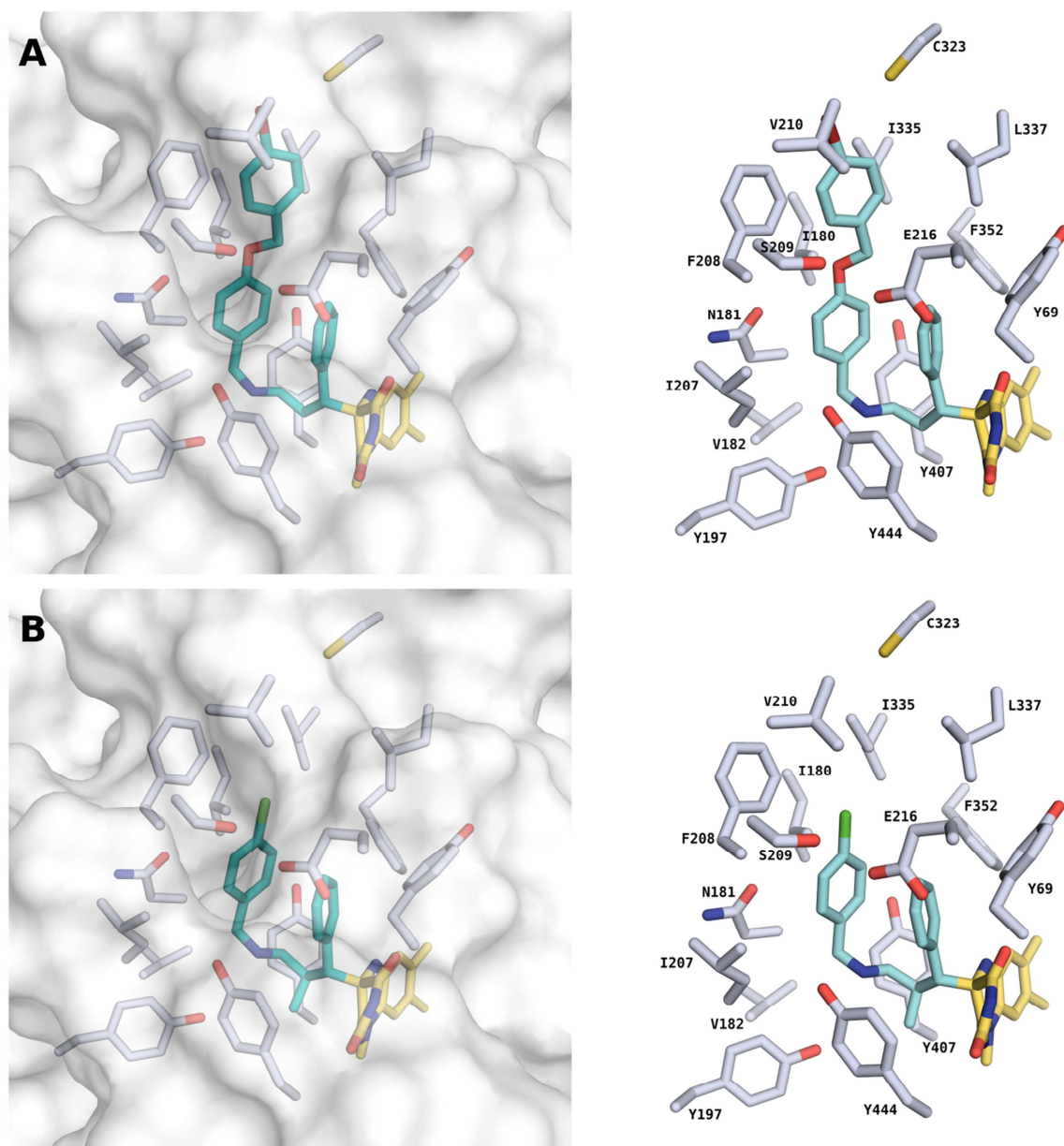
In contrast to MAOs, LSD1 shows a wide active site cleft ( $\sim 550 \text{ \AA}^3$  and  $\sim 400 \text{ \AA}^3$  in MAOs[49], respectively, compared to  $\sim 1245 \text{ \AA}^3$  in LSD1[50]), which allows the binding of the modelled C4a adducts in an extended conformation, as exemplified by the binding modes of **7v**, **7ah**, **7r**, and **8c** (Figure 4A-D). The 2-phenyl moiety adopts the same position as observed in the crystal structure of analogous 1-ethyl-2-PCPA (PDB ID 4UV8) and is embedded in a hydrophobic region undergoing hydrophobic interactions with Phe538 and Val333. Meanwhile, the *N*-substituent is hosted either in a sub-pocket lined by Asn540, Trp552, Val764, Tyr773, Pro808, and Ala809 (**7v** Figure 4A), or in an adjacent sub-pocket formed by Thr335, Asp555, Glu559, Phe560, and Tyr807 (**7ah** Figure 4B). The docking poses of derivatives bearing hydrophobic and polar substituents, as exemplified by **7r** and **8c** respectively, are shown in Figure 4C and 4D. While the biphenyl group of **7r** is able to form van-der-Waals (vdW) interactions with Phe560, the polar sulfonamide group of **8c** undergoes polar interactions and forms two H-bonds with the side chains of His812 and Asp555. This might explain why LSD1 can tolerate both polar and apolar moieties at the *N*-benzyl substituent. The obtained docking results also demonstrate that an additional methyl group in 2-PCPA would cause a steric clash, especially with Thr810 and, thus, disrupt the formation of the observed binding mode. This might explain the lack of activity of the reported 2-methyl-3-phenylcyclopropan-1-amine derivatives on LSD1.





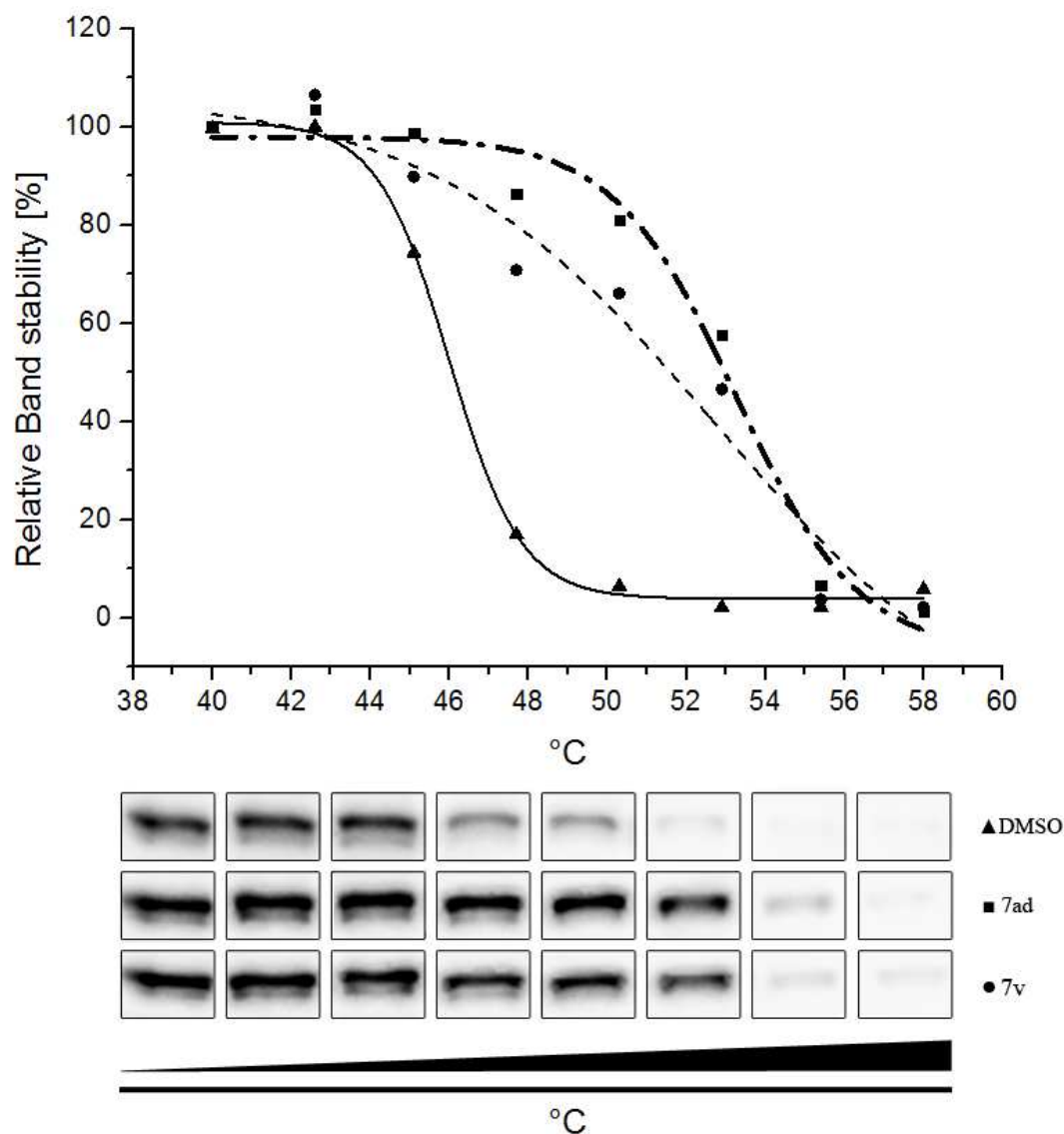
**Figure 4.** Selected docking poses of the modelled C4a-adducts in LSD1. The surface of the protein is depicted on the left side and removed on the right side for more clarity. The protein residues are shown as white sticks. The adduct is displayed as cyan and yellow sticks, for the ligand and the flavin ring of FAD, respectively. Water molecules are shown as red spheres; **(A)** Docking pose of **7v** C4a-adduct in LSD1; **(B)** Docking pose of **7ah** C4a-adduct in LSD1; **(C)** Docking pose of **7r** C4a-adduct in LSD1; **(D)** Docking pose of **8c** C4a-adduct in LSD1.

MAO-A possesses a relatively narrow active site cleft, which can still host the C4a adducts of described *N*-benzyl-PCPA derivatives, albeit in a U-shaped conformation (Figure 5). Again, the 2-phenyl group is embedded in a hydrophobic region, where it undergoes vdW interactions with Tyr69 and Phe352. In contrast to the binding mode predicted in LSD1, the substituent at the *N*-benzyl group of the studied compounds is hosted in a notably hydrophobic region and surrounded by the residues Ile180, Phe208, Val210, Cys323, Ile335, and Leu337. Hence, a polar substituent at the benzyl group would be highly unfavorable, which explains the selectivity of the sulfonamide derivatives **8c** and **8d** for LSD1 over MAO-A. The derived docking results also supported the notion that MAO-A can host 2-Methyl-3-phenylcyclopropan-1-amine derivatives, as exemplified by the docking pose of **6c** in MAO-A (Figure 5B). The obtained docking pose shows a highly similar binding mode as for the unsubstituted derivatives, with the 2-methyl group placed in the vicinity of Tyr444.



**Figure 5.** Selected docking poses of C4a-adducts in MAO-A. The surface of the protein is depicted on the left side and removed on the right side for more clarity. The protein residues are shown as white sticks. The adduct is displayed as cyan and yellow sticks, for the ligand and flavin ring of FAD, respectively. Water molecules are shown as red spheres; **(A)** Docking pose of **7ag** C4a-adduct in MAO-A; **(B)** Docking pose of **6c** C4a-adduct in MAO-A.

As it has been shown that LSD1 inhibition does not generally lead to global hypermethylation in leukemic cells[51, 52], we sought to demonstrate target engagement by alternative means using a binding assay which is independent from putative downstream signaling effects. One approach to measure target binding in a cellular setting is the Cellular Thermal Shift Assay (CETSA). Treated cells with and without inhibitor are stressed thermally and binding to the target might lead to a thermostabilization of the target in question.[53] In the assay only the intended target protein is monitored and possible off-targets of analyzed compounds would stay unnoticed. First, we realized a well-defined “melting curve” of LSD1 in THP-1 cells, using western blotting as a means of quantification of LSD1 in the supernatant of lysates of cells after thermal stress. Incubation of the cells with the positive control **1b** ( $T_m = 50.8 \pm 0.5$  °C) and the inhibitors **7v** ( $T_m = 52.8 \pm 2.9$  °C) and **7ad** ( $T_m = 53.2 \pm 0.7$  °C) showed a strong right shift of the melting curve (DMSO control  $T_m = 46.0 \pm 1.1$  °C; mean and standard deviation calculated from four independent experiments). The investigated negative controls **6c** ( $T_m = 47.9 \pm 0.4$  °C) and **6e** ( $T_m = 45.6 \pm 0.3$  °C) did not show a strong shift of the melting curve. This strongly supports LSD1 target engagement in these cells (Figure 6, S4-S9) but also the usefulness of the negative controls **6c** and **6e** for target engagement studies of LSD1.

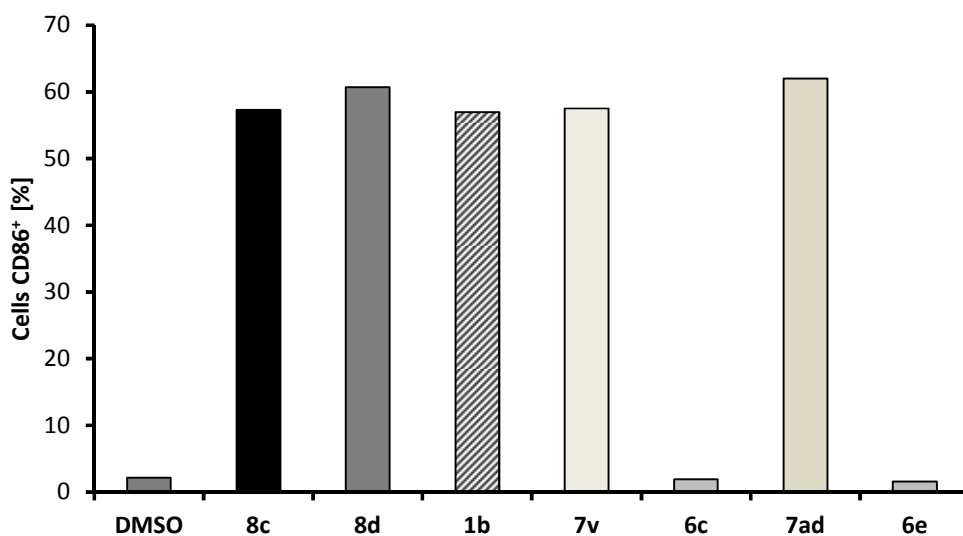


**Figure 6.** **7v** and **7ad** stabilize LSD1 at elevated temperatures and lead to a thermal shift upon ligand binding. Curves were fitted with a Boltzmann fit.

We also investigated the cellular activity of the LSD inhibitors on rhabdomyosarcoma cells that are reported to harbor high levels of LSD1.[54, 55] However, treatment with compounds **1c**, **8c** and **8d** induced a limited amount of cell death even at high concentrations (Figure S3 A). As

we recently found that LSD1 inhibition can enhance HDAC inhibitor-induced cell death in rhabdomyosarcoma cells[56], we also combined compounds **1c**, **8c** and **8d** with the second generation HDAC inhibitor JNJ-26148515. Notably, all three LSD1 inhibitors significantly enhanced JNJ-26148515-induced cell death in rhabdomyosarcoma cells (Figure S3 B).

In addition to this, we determined whether **7ad**, **7v** and the selective inhibitors **8c** and **8d** can induce the expression of the cell surface marker CD86<sup>+</sup> in leukemic cells, the negative controls **6c** and **6e** were also included in the assay. This immunoglobulin can be found e.g. on monocytes, dendritic cells, macrophages, and its gene is up-regulated upon LSD1-inhibition. We could show that the inhibitors increase the expression to a similar level, compared to the reference inhibitor **1b** (Figure 7). The negative controls **6c** and **6e** consistently also did not alter CD86<sup>+</sup> expression on THP-1 cells compared to the vehicle treated cells. **1b** has already been used in our CFU assay (also **7ad**, **7v** and **6c**, **6e**) and in the literature for these experiments.[57] We conclude that our compounds exhibit a clear and significant anti-cancer effect regarding clonogenic potential and cell differentiation in leukemic THP-1 cells.



**Figure 7.** Induced expression of CD86<sup>+</sup> surface marker in AML THP-1 cells by selected compounds at 0.5  $\mu$ M. Depicted results are representative out of 3 independent measurements. All performed experiments with active inhibitors showed clear increase in CD86<sup>+</sup> expression level upon treatment compared to vehicle treated cells. The negative controls **6c** and **6e** did not increase the expression of CD86<sup>+</sup>. The precise CD86<sup>+</sup> expression level of THP-1 cells is passage number-related.[58]

### Conclusion

Here, we present the SAR of *N*-benzyl derivatives of *trans*-2-phenylcyclopropylamine (**1a**) as inhibitors of LSD1. Some related compounds from other groups (**1c**, **1d**) are undergoing clinical trials for the treatment of leukemia but SAR studies of this class have not been presented in detail in the peer-reviewed literature.

We provide evidence in contrast to a common notion that potent LSD1 inhibitors would not be in need of a polar or basic functionality on the *N*-substituent. Yet, we show that the lipophilic compounds are also quite strong inhibitors of MAOs. This might still be of interest, as dual-specific LSD1/MAO-B-inhibitors have been postulated to possess great potential for the treatment of neurodegenerative disorders.[59, 60] In this case, the more lipophilic nature of the compounds would also be beneficial for CNS penetration.

Further extension of our structure-activity studies towards polar substituents led to the identification of inhibitors that are potent in blocking LSD1 and selective over MAOs. We found that (i) halides improve the potency, (ii) bulky moieties are preferred in *meta* substitution and (iii) polar groups improve potency and selectivity. Docking studies suggest that the wide binding pocket of LSD1 can accommodate alternative binding interactions for lipophilic vs. polar

interactions whereas e.g in MAO-A the binding site is more narrow and mostly lipophilic. This explains the selectivity of inhibitors with polar substituents. Both unselective and selective inhibitors showed strong reduction in the clonogenic potential of leukemic cells in CFU assays, thus showing a LSD1 inhibitory phenotype in cells.

To show cellular target engagement, we have established a CETSA assay for LSD1. This method works in a native background and has been used for other epigenetic targets [61, 62] and in a dose dependent assay for LSD1 successfully before.[63] The investigated trimethylated cyclopropylamine molecules (e.g. **6c** and **6e**) can be used as structurally closely related negative controls for biological studies for *trans*-2-PCPA-based LSD1 inhibition studies and development of novel assays. Thus, we present a significant methodological advantage for further studies of LSD1 inhibitors and guide further optimization of either selective or dual-specific LSD1 inhibitors based on the *trans*-2-PCPA scaffold.

## Materials and Methods

**General information.** Reactions were performed using a magnetic hot plate stirrer (*Heidolph*) utilizing an aluminum heating block at elevated temperature. Solvents and the starting materials (chemicals) were purchased from commercial sources and were used without further purification. Analytical TLC was performed with TLC silica gel 60 F<sub>254</sub> plates from Merck. All yields reported are isolated yields after removal of residual solvents. NMR spectra (<sup>1</sup>H NMR: 400 MHz; <sup>13</sup>C NMR: 100 MHz) were obtained on a *Bruker* Avance DRX magnetic resonance spectrometer at room temperature. Spectra are reported as chemical shifts in parts per million (ppm) relative to the residual non-deuterated components of NMR solvents (DMSO-*d*<sub>6</sub>: <sup>1</sup>H δ = 2.50, <sup>13</sup>C δ = 39.52; CDCl<sub>3</sub>: <sup>1</sup>H δ = 7.26, <sup>13</sup>C δ = 77.16; Deuterium oxide: <sup>1</sup>H δ =

4.79).[64] Proton coupling patterns were described as singlet (s), doublet (d), doublet of doublets (dd), doublet of doublets of doublets (ddd), doublet of triplets (dt), triplet (t), triplet of doublets (td), quartet (q), multiplet (m) or broad singlet (bs). Signals which could not be identified in  $^{13}\text{C}$  NMR but were detected in HBMC are marked with (\*). Mass spectra were recorded with TSQ700 *Thermoelectron* spectrometers using APCI ( $\text{NH}_3$ ) and ESI. Compounds were purified by flash column chromatography on a *Biotage Isolera One*, eluting with a gradient of ethyl acetate/cyclohexane or acetonitrile/water without additives. The purity of the final compounds was determined by HPLC with UV-detection at 210 nm. HPLC were performed on an Agilent Technologies HPLC system Infinity 1260, using Kinetex XB-C18, 5  $\mu\text{m}$ , 100  $\text{\AA}$  250 x 4.6 mm (*Phenomenex*). Elution was performed at room temperature under gradient conditions. Eluent A was  $\text{H}_2\text{O}$  containing 0.05 % 2,2,2-trifluoroacetic acid (TFA). Eluent B was acetonitrile (ACN), also containing 0.05 % TFA. Linear gradient conditions were as follows: 0–4 min, A = 90 %, B = 10 %; 4–29 min, linear increase to B = 100 %; 29–31 min, B = 100 %; 31–40 min, A = 10 %, B = 90 %. A flow rate of  $1.0 \text{ mL}\cdot\text{min}^{-1}$  was maintained. The purity of all final compounds was >95 %. Semi preparative HPLC has been performed on the same HPLC system at room temperature under gradient conditions. Eluent C was *n*-hexane; Eluent D was isopropanol, both without additives. Linear gradient conditions: 0–4 min, C=90 %, D=10 %; 4–17 min, linear decrease to C=72 %; 17–20 min, C=50 %, D=50 %; 20–22 min C=90 %, D=10 %. A Lux Cellulose-1, 5  $\mu\text{m}$ , 1000  $\text{\AA}$ , 250 x 10.0 mm column (*Phenomenex*) was used with a flow rate of  $5 \text{ mL}\cdot\text{min}^{-1}$  during the entire elution. Optical purity of the enantiomers has been analyzed on a Lux® Cellulose-1, 5  $\mu\text{m}$ , 1000  $\text{\AA}$ , 250 x 4.6 mm column with the same gradient conditions as above, and a flow rate of  $1 \text{ mL}\cdot\text{min}^{-1}$  during the entire elution. All IR/VCD spectra (resolution:  $4 \text{ cm}^{-1}$ ) were recorded on a Tensor 27 FT-IR spectrometer (*Bruker*) equipped with a PMA 50

VCD side bench (retardation of the photoelastic modulator:  $\frac{1}{4} \lambda$  at  $1400 \text{ cm}^{-1}$ , frequency: 50 kHz; *Bruker*).

**General Procedure A (Cyclopropanation).** The appropriate styrene derivative (1.0 eq.) was dissolved in dry 10 mL DCM in presence of Cu(II)acetylacetonate (0.05 eq.) and treated slowly with (1.5 eq.) ethyl diazoacetate over 4 h at  $60 \text{ }^\circ\text{C}$ . The reaction mixture was filtered, concentrated in vacuo and purified using flash chromatography (silica gel; cyclohexane/ethyl acetate) to afford the title compound as *cis* and *trans* isomers.

**General Procedure B (Ester hydrolysis).** The appropriate ester (1 eq.) and 5 eq. of an aqueous KOH solution were dissolved in methanol. The reaction mixture was stirred over night at room temperature and monitored by TLC. After the reaction was finished, methanol was evaporated and the aqueous phase extracted three times with 25 mL ethyl acetate. The organic layers were separated, dried over anhydrous  $\text{Na}_2\text{SO}_4$  and concentrated in vacuo to afford the pure title carboxylic acid.

**General Procedure C (Curtius rearrangement).** A solution of triethylamine (4.0 eq.), diphenylphosphoryl azide (1.5 eq.) and the appropriate carboxylic acid (1.0 eq.) was stirred in *tert*-butanol (20 eq.) at  $50 \text{ }^\circ\text{C}$  for 6 h under nitrogen atmosphere before increasing the temperature to  $120 \text{ }^\circ\text{C}$  for a duration of 12 h. Thereafter, 1.5 eq. of di-*tert*-butyldicarbonate was added to the reaction mixture, which was kept stirring for another 2 h. It was quenched with 20 mL of an aqueous (5 %)  $\text{NaHCO}_3$  solution and the organic solvent was evaporated *in vacuo*. Upon completion, the aqueous phase was extracted three times with 20 mL of ethyl acetate, dried over anhydrous  $\text{Na}_2\text{SO}_4$ , concentrated in vacuo and purified using flash chromatography (silica gel; cyclohexane/ethyl acetate) to yield the title compound.

**General Procedure D (Deprotection of Boc-protected amines).** The carbamate was dissolved in 5 mL 1,4-dioxane with an excess of 2 M hydrochloric acid solution. The reaction mixture was kept stirring over night at room temperature. The formed precipitate was filtered and washed with diethyl ether to afford the pure titled compound.

**General Procedure E (Reductive Amination).** *Trans*-2-phenylcyclopropylamine hydrochloride (1.0 eq.), acetic acid (1.0 eq.) and the appropriate aldehyde (0.9 eq.) were dissolved in a round bottom flask in 10 mL dry DCE. The reaction mixture was stirred gently at room temperature for 2 h, before sodium triacetoxyborohydride (3.0 eq.) was added in small portions to the reaction vessel. The reaction was monitored by TLC and quenched using 10 mL of an aqueous (5 %) NaHCO<sub>3</sub> solution. The organic layer was separated and the aqueous layer extracted three times with 10 mL DCE. All organic layers were combined, dried over anhydrous Na<sub>2</sub>SO<sub>4</sub>, concentrated in vacuo and purified using flash chromatography (silica gel; cyclohexane/ethyl acetate) to give the desired compound.

**Fluorescence based LSD1 assay.** Enzyme activity and inhibition was performed in an established HRP-coupled assay system based on the Amplex Red protocol from Invitrogen (*BPS Bioscience*). The assay was measured in a white 384-well OptiPlate (*PerkinElmer*) using 0.92 µg of LSD1 enzyme (expressed in Sf9 cells as published elsewhere[65]), and 2 µl of inhibitor (in DMSO, or DMSO as a control without inhibitor). This 10 µL solution was incubated for 15 min. Demethylation reaction was initiated by adding 10 µL of an aliquot of H3K4<sub>aa1-20</sub> (final peptide concentration 77 µM. The solution was diluted in reaction buffer 45 mM HEPES, 40 mM NaCl, pH = 8.5; sequence: ARTK<sub>(me2)</sub>QTARKSTGGKAPRKQL; from *Peptide Specialty Laboratories Ltd.*). Buffer solution without peptide was used as blanks. The plate was incubated for 60 min at room temperature. Thereafter 20 µl of Amplex Red mixture (final concentration 50 µM Amplex

Red reagent and 1 U/mL HRP in reaction buffer) were added. Fluorescence was detected on a polarstar microplate reader ( $\lambda_{\text{ex}}$ : 510 nm,  $\lambda_{\text{em}}$ : 615 nm; *BMG*).

**Luminescent based MAO assay.** Enzyme activity and inhibition was performed using a commercial assay kit MAO-Glo (Promega) in a final volume of 20  $\mu\text{L}$ . 0.62  $\mu\text{g}$  MAO-A or 3.25  $\mu\text{g}$  MAO-B enzyme (*Sigma*) and the inhibitor in 2  $\mu\text{L}$  DMSO (or DMSO as a control without inhibitor) were incubated at r.t. for 15 min, before the reaction was conducted at 30 °C for 60 min after addition of a luminogenic MAO substrate ( $K_m = 40 \mu\text{M}$  for MAO-A or 4  $\mu\text{M}$  for MAO-B as final concentration). A 20  $\mu\text{L}$  of a luciferin detection reagent was added to stop the enzymatic activity. The assay read-out has been executed in an EnVision 2102 Multilabel Reader (*Perkin Elmer*) 20 min after the reaction was mixed with the detection reagent.

**Cell Culture.** THP-1 (RRID:CVCL\_0006) cells for CFU assay were kindly provided by Prof. Lübbert and cultivated in RPMI1640 medium supplemented with 10 % (v/v) FCS, 2 mM L-glutamine, 1 % Penicillin/Streptomycin, under  $\text{CO}_2$  atmosphere (5 %) at 37 °C. Murine bone marrow cells were isolated from C57BL6/J mice by flushing femora and tibiae with Dulbecco's phosphate-buffered saline (DPBS) supplemented with 2 % fetal bovine serum (FBS).

Lineage negative (Lin-) hematopoietic progenitors were separated using the Lineage Cell Depletion Kit (Miltenyi Biotech) according to manufacturer's instructions. Lin- progenitors were cultured in Dulbecco's modified Eagle medium (DMEM) supplemented with 15 % FBS, 10  $\text{ng}\cdot\text{mL}^{-1}$  human IL-6, 10  $\text{ng}\cdot\text{mL}^{-1}$  murine IL-3, and 100  $\text{ng}\cdot\text{mL}^{-1}$  murine stem cell factor (*Peptotech*).

RH30 cells were obtained from the *Deutsche Sammlung von Mikroorganismen und Zellkulturen GmbH*. Cells were maintained in RPMI 1640 (*Life Technologies Inc.*) supplemented

with 10 % fetal calf serum (FCS), 1 % Penicillin/Streptomycin and 1 mM sodium pyruvate (*Invitrogen*).

**CETSA.** 10 mL THP-1 cells were cultured in T-75 flasks at a density of  $2 \cdot 10^6$  cells·mL<sup>-1</sup> and treated with DMSO (final concentration 0.3 % (v/v)) or inhibitor (final concentration 30  $\mu$ M) at 37 °C for 1 hour. After treatment, cells were centrifuged at  $500 \times g$  for 5 min at room temperature and washed with PBS. Cells were resuspended in 500  $\mu$ L PBS with protease inhibitor cocktail (Roche, complete tablets, EDTA-free). The cell suspension was equally aliquoted into 8 PCR tubes each with 25  $\mu$ L and heated for 3 min to 40, 42.6, 45.1, 47.7, 50.3, 52.9, 55.4 or 58 °C followed by cooling for 3 min at 25 °C. Subsequently cells were lysed using liquid nitrogen and three repeated freeze–thaw cycles (thawing at 25 °C). Cell debris and precipitated proteins were separated by centrifugation at  $20000 \times g$  for 20 min at 4 °C. The supernatants were transferred to new microtubes and analyzed by sodium dodecyl sulfate polyacrylamide gel electrophoresis (SDS-PAGE) followed by western blot analysis (1° antibody: ab37165 (*Abcam*)).

**CFU.** 2.4 mL MethoCult H4230 (*StemCell Technologies*) aliquots, prepared as described by the manufacturer, were supplemented with 300  $\mu$ L FCS, 300  $\mu$ L IMDM (Iscove's Modified Dulbecco's Medium; *StemCell Technologies*) and vehicle or inhibitor solution was added to a final conc. of 0.5 % DMSO and vigorously mixed. After incubation at room temperature for 5 min to allow bubbles rise to the top, 500 cells in 300  $\mu$ L IMDM supplemented with 2 % (v/v) FCS were added to each aliquot. Samples were vigorously mixed, incubated at room temperature for 5 min and aliquoted in 1.1 mL aliquots in two TC dishes ( $\varnothing$ 35 mm; *Sarstedt*). TC dishes were placed together with a third dish ( $\varnothing$ 35 mm; *Greiner bio-one*), containing 3 mL sterile water, in a

TC dish ( $\text{\O}100$  mm; *Sarstedt*) and incubated in a 5 %  $\text{CO}_2$  atmosphere at 37 °C for 10 days. Colonies were counted by a light microscopy (*Zeiss PrimoVert*).

**FACS Analysis.** THP-1 cells were diluted to  $1 \cdot 10^5$  cells $\cdot$ mL<sup>-1</sup> and inhibitor or vehicle was added to a final concentration of 0.1 % DMSO. After 72 h cells were washed twice with FACS-buffer (PBS + 1 % BSA) and stained with allophycocyanin (APC)-conjugated anti-human CD86 antibodies (*BD Bioscience*) for 15 min at room temperature. Cells were washed and stained with 7-AAD (*BD Bioscience*) for apoptosis analysis. Measurement was done using a CyAn (*Beckmann Coulter*) with 104 events per sample. Gates were set using unstained and single stained and single stained vehicle treated cells.

**Transformation of primary murine progenitor cells by retroviral overexpression of Hoxa9 and Meis1.** In order to induce retroviral overexpression of Hoxa9 and Meis1, Lin-progenitors were co-cultured with GP+E-86 (ATCC) virus producer cells for 48 h containing MSCV-Hoxa9-pgk-neomycin (Hoxa9<sup>neo</sup>)[66] and MSCV-HA-Meis1aIRES-YFP[67]. 10 ng $\cdot$ mL<sup>-1</sup> Polybrene (*Sigma*) was used to increase transduction efficiency. Infected cells were sorted for positive YFP signal using a BD FACSAria III cell sorter and further selection was performed in media supplemented with 0.6  $\mu$ g $\cdot$  $\mu$ L<sup>-1</sup> G418 (*Sigma*).

**Flow Cytometry.** Flow cytometric analysis were performed after treatment with indicated concentrations of LSD1 inhibitors **7v** and **7ad** for 96 h. Cells were analyzed for expression of cell surface marker using a BD LSRFortessa cytometer. Cells were stained with allophycocyanin (APC)-conjugated anti-mouse CD117 (c-Kit) antibodies and phycoerythrin cyanine 7 (PE-Cy7)-conjugated anti-mouse Ly-6A/E (Sca1) antibodies (*eBiosciences*) in PBS containing 2 % FBS at 4 °C for 30 min. Cells were then washed and 20000 events were acquired. The analysis was done with FlowJo Software Version 10.

**Statistical analysis.** Statistical analysis was performed using GraphPad Prism 7 Software. Student's t-test was used to compare averages of treated groups with control groups and to calculate the p value.

**Cell death determination.** Cell death was assessed by propidium iodide (PI)/HOECHST staining to determine plasma membrane permeability using ImageXpress® Micro XLS system (*Molecular Devices, LLC*) according to the manufacturer's instructions.

**VCD measurements.** An enantiomer of the free base of **1a** was placed as neat liquid in a rotatable BaF<sub>2</sub> cell with a pathlength of 6 μM. The accumulated measurement time was 12 h. The experimental spectra were obtained by averaging the recorded spectra and subtraction of the spectrum of racemic tranylcypromine.

A 100 mM solution of *trans-N*-(3-nitrobenzyl)-2-phenylcyclopropan-1-amine (*S,R*)-**7ad** or (*R,S*)-**7ad** in anhydrous CDCl<sub>3</sub> was placed in a rotatable BaF<sub>2</sub> cell with a pathlength of 110 μM. The presented experimental spectra represent 6 h of measuring after subtraction of the solvent spectrum.

**Quantum chemical calculations.** The MMFF-based conformer search algorithm in Spartan '08 software (*Wavefunction Inc.*) delivered 3 conformers for **1a** and 11 conformers for *trans-N*-(3-nitrobenzyl)-2-phenylcyclopropan-1-amine (**7ad**). Geometry optimization and IR/VCD calculations were carried out at the DFT level (B3LYP/6-311++G(d,p)) in Gaussian 09D.[68] Frequencies of the calculated spectra were scaled by 0.977 determined with the scale factor optimization tool in CDspecTech.[69] Theoretical spectra are shown as the Boltzmann-weighted average of the single calculated spectra with Lorentzian lineshapes of 6 cm<sup>-1</sup> bandwidth around the calculated intensities.

**Molecular docking. Ligand preparation.** The C4a-adducts of the studied compounds with FAD were generated using MOE[70] (version 2014.09, Chemical Computing Group, Montreal, Canada) taking the flavin ring of FAD from the crystal structure (PDB ID 4UV8). The generated ligands were then cured using LigPrep[71] as implemented in the *Schrödinger* suite; protonation states were assigned at pH 7±1 using Epik, tautomeric forms as well as possible conformations were generated and energy minimized using the OPLS force field. Subsequently, 20 low energy conformers were generated using the program OMEGA[72-74] as implemented in the *OpenEye* suite.

**Protein preparation.** The crystal structures of LSD1 (PDB ID: 4UV8)[28] and MAO-A (PDB ID: 3BXS)[46] were used for the docking studies. The protein structures were prepared with *Schrödinger's* Protein Preparation Wizard[74]: Hydrogen atoms were added and the H-bond network was subsequently optimized. The protonation states at pH 7.0 were predicted using the PROPKA tool in *Schrödinger*. The structures were finally subjected to a restrained energy minimization step using the OPLS2005 force field (RMSD of the atom displacement for terminating the minimization was 0.3 Å). Only one conserved water molecule (HOH2003) was kept in the crystal structure of LSD1 (PDB ID: 4UV8) during the docking procedure, while all water molecules were deleted from the crystal structure of MAO-A.

**Docking.** The receptor grid preparation for the docking procedure was carried out by assigning the cut co-crystallized ligand (only the flavin ring was kept in FAD) as the centroid of the grid box. Molecular docking was performed using Glide[48] (*Schrödinger Inc.*, New York, USA) in the Standard Precision mode, while using a positional constraint for the flavin ring (1 Å allowed deviation). A total of 20 poses per ligand conformer were included in the post-docking minimization step and a maximum of two docking poses were stored for each ligand conformer.

**PAINS Analysis.** All compounds were filtered for pan-assay interference compounds (PAINS)[75] using the online filter <http://zinc15.docking.org/patterns/home/>. Only compound **7t** was flagged as PAINS. We choose not to investigate this compound further with regard to mechanistic studies as it is not crucial for SAR and the activity of the general class is well documented.

**Supporting Information.** Detailed experimentals of compounds, NMR spectra, VCD spectra

### **Corresponding Author**

\*Prof. Dr. Manfred Jung, Institute of Pharmaceutical Sciences, University of Freiburg, Albertstr. 25, 79104 Freiburg, Germany, email: [manfred.jung@pharmazie.uni-freiburg.de](mailto:manfred.jung@pharmazie.uni-freiburg.de), Tel. 0049-761-203-6335, Fax -6351.

### **Author Contributions**

The manuscript was written through contributions of all authors. All authors have given approval to the final version of the manuscript.

### **Funding Sources**

Financial support of this work by the DFG (RTG 1976 and SFB 992, projects A04, B01 and C04) is gratefully acknowledged; R.S. further thanks the European Research Council [ERC AdGrant 322844], the Deutsche Forschungsgemeinschaft [CRC 850, CRC746 and Schu688/12–1].

### **Acknowledgment**

This research was supported in part by the bwHPC initiative and the bwHPC-C5 project provided through associated compute services of the JUSTUS HPC facility at the University of

Ulm. W. Sippl and D. Robaa thank the OpenEye Free Academic Licensing Program for providing a free academic license for molecular modeling and chemoinformatics software.

ACCEPTED MANUSCRIPT

## REFERENCES

- [1] E. Metzger, M. Wissmann, N. Yin, J.M. Muller, R. Schneider, A.H. Peters, T. Gunther, R. Buettner, R. Schule, LSD1 demethylates repressive histone marks to promote androgen-receptor-dependent transcription, *Nature*, 437 (2005) 436-439.
- [2] Y. Shi, F. Lan, C. Matson, P. Mulligan, J.R. Whetstone, P.A. Cole, R.A. Casero, Y. Shi, Histone demethylation mediated by the nuclear amine oxidase homolog LSD1, *Cell*, 119 (2004) 941-953.
- [3] Y. Wang, H. Zhang, Y. Chen, Y. Sun, F. Yang, W. Yu, J. Liang, L. Sun, X. Yang, L. Shi, R. Li, Y. Li, Y. Zhang, Q. Li, X. Yi, Y. Shang, LSD1 is a subunit of the NuRD complex and targets the metastasis programs in breast cancer, *Cell*, 138 (2009) 660-672.
- [4] M. Wang, X. Liu, G. Jiang, H. Chen, J. Guo, X. Weng, Relationship between LSD1 expression and E-cadherin expression in prostate cancer, *Int Urol Nephrol*, 47 (2015) 485-490.
- [5] L. Chen, Y. Xu, B. Xu, H. Deng, X. Zheng, C. Wu, J. Jiang, Over-expression of lysine-specific demethylase 1 predicts tumor progression and poor prognosis in human esophageal cancer, *Int J Clin Exp Pathol*, 7 (2014) 8929-8934.
- [6] W.J. Harris, X. Huang, J.T. Lynch, G.J. Spencer, J.R. Hitchin, Y. Li, F. Ciceri, J.G. Blaser, B.F. Greystoke, A.M. Jordan, C.J. Miller, D.J. Ogilvie, T.C. Somerville, The histone demethylase KDM1A sustains the oncogenic potential of MLL-AF9 leukemia stem cells, *Cancer Cell*, 21 (2012) 473-487.
- [7] A. Sprussel, J.H. Schulte, S. Weber, M. Necke, K. Handschke, T. Thor, K.W. Pajtler, A. Schramm, K. Konig, L. Diehl, P. Mestdagh, J. Vandesompele, F. Speleman, H. Jastrow, L.C. Heukamp, R. Schule, U. Duhrsen, R. Buettner, A. Eggert, J.R. Gothert, Lysine-specific demethylase 1 restricts hematopoietic progenitor proliferation and is essential for terminal differentiation, *Leukemia*, 26 (2012) 2039-2051.
- [8] T. Kouzarides, Chromatin modifications and their function, *Cell*, 128 (2007) 693-705.
- [9] T. Jenuwein, C.D. Allis, Translating the histone code, *Science*, 293 (2001) 1074-1080.
- [10] N.T. Tomita, D.; Tominari, Y.; Imamura, S.; Morimoto, S.; Kojima, T.; Toyofuku, M.; Hattori, Y.; Kaku, T.; Ito, M., Preparation of cyclopropanamines and their use for prevention and treatment of schizophrenia, Alzheimer's disease, Parkinson's disease, and Huntington chorea, WO2014058071, (2014).
- [11] R. Neelamegam, E.L. Ricq, M. Malvaez, D. Patnaik, S. Norton, S.M. Carlin, I.T. Hill, M.A. Wood, S.J. Haggarty, J.M. Hooker, Brain-penetrant LSD1 inhibitors can block memory consolidation, *ACS Chem Neurosci*, 3 (2012) 120-128.
- [12] N.W. Johnson, J. Kaspavec, W.H. Miller, M.B. Rouse, D. Suarez, X. Tian, Preparation of cyclopropylamines as LSD1 inhibitors in the treatment of cancer, WO2012135113A, (2012).
- [13] T. Maes, I. Tirapu, C. Mascaró, A. Ortega, A. Estiarte, N. Valls, J. Castro-Palomino, C.B. Arjol, G. Kurz, Preclinical characterization of a potent and selective inhibitor of the histone demethylase KDM1A for MLL leukemia, ASCO Annual Meeting, (2013).
- [14] L. Morera, M. Lubbert, M. Jung, Targeting histone methyltransferases and demethylases in clinical trials for cancer therapy, *Clin Epigenetics*, 8 (2016) 57.
- [15] Press Release, Oryzon Genomics, [www.oryzon.com](http://www.oryzon.com), 2017.
- [16] H. Benelkebir, C. Hodgkinson, P.J. Duriez, A.L. Hayden, R.A. Bulleid, S.J. Crabb, G. Packham, A. Ganesan, Enantioselective synthesis of tranlylcypromine analogues as lysine demethylase (LSD1) inhibitors, *Bioorg Med Chem*, 19 (2011) 3709-3716.

- [17] R. Ueda, T. Suzuki, K. Mino, H. Tsumoto, H. Nakagawa, M. Hasegawa, R. Sasaki, T. Mizukami, N. Miyata, Identification of cell-active lysine specific demethylase 1-selective inhibitors, *J Am Chem Soc*, 131 (2009) 17536-17537.
- [18] Y. Liang, D. Quenelle, J.L. Vogel, C. Mascaro, A. Ortega, T.M. Kristie, A novel selective LSD1/KDM1A inhibitor epigenetically blocks herpes simplex virus lytic replication and reactivation from latency, *MBio*, 4 (2013) e00558-00512.
- [19] T. Kakizawa, Y. Ota, Y. Itoh, H. Tsumoto, T. Suzuki, Histone H3 peptide based LSD1-selective inhibitors, *Bioorg Med Chem Lett*, 25 (2015) 1925-1928.
- [20] Y. Ota, Y. Itoh, A. Kaise, K. Ohta, Y. Endo, M. Masuda, Y. Sowa, T. Sakai, T. Suzuki, Targeting Cancer with PCPA-Drug Conjugates: LSD1 Inhibition-Triggered Release of 4-Hydroxytamoxifen, *Angew Chem Int Ed Engl*, 55 (2016) 16115-16118.
- [21] S. Mimasu, T. Sengoku, S. Fukuzawa, T. Umehara, S. Yokoyama, Crystal structure of histone demethylase LSD1 and tranlycypromine at 2.25 Å, *Biochem Biophys Res Commun*, 366 (2008) 15-22.
- [22] C. Binda, S. Valente, M. Romanenghi, S. Pilotto, R. Cirilli, A. Karytinis, G. Ciossani, O.A. Botrugno, F. Forneris, M. Tardugno, D.E. Edmondson, S. Minucci, A. Mattevi, A. Mai, Biochemical, structural, and biological evaluation of tranlycypromine derivatives as inhibitors of histone demethylases LSD1 and LSD2, *J Am Chem Soc*, 132 (2010) 6827-6833.
- [23] D. Dhanak, Drugging the cancer epigenome [abstract], in Proceedings of the 104th Annual Meeting of the American Association for Cancer Research, AACR, Washington, DC, Philadelphia (PA) **2013**.
- [24] W. Fiskus, S. Sharma, B. Shah, B.P. Portier, S.G. Devaraj, K. Liu, S.P. Iyer, D. Bearss, K.N. Bhalla, Highly effective combination of LSD1 (KDM1A) antagonist and pan-histone deacetylase inhibitor against human AML cells, *Leukemia*, 28 (2014) 2155-2164.
- [25] L.Y. Ma, Y.C. Zheng, S.Q. Wang, B. Wang, Z.R. Wang, L.P. Pang, M. Zhang, J.W. Wang, L. Ding, J. Li, C. Wang, B. Hu, Y. Liu, X.D. Zhang, J.J. Wang, Z.J. Wang, W. Zhao, H.M. Liu, Design, synthesis, and structure-activity relationship of novel LSD1 inhibitors based on pyrimidine-thiourea hybrids as potent, orally active antitumor agents, *J Med Chem*, 58 (2015) 1705-1716.
- [26] C.J. Kutz, S.L. Holshouser, E.A. Marrow, P.M. Woster, 3,5-Diamino-1,2,4-triazoles as a novel scaffold for potent, reversible LSD1 (KDM1A) inhibitors, *Medchemcomm*, 5 (2014) 1863-1870.
- [27] D.M. Gooden, D.M. Schmidt, J.A. Pollock, A.M. Kabadi, D.G. McCafferty, Facile synthesis of substituted trans-2-arylcyclopropylamine inhibitors of the human histone demethylase LSD1 and monoamine oxidases A and B, *Bioorg Med Chem Lett*, 18 (2008) 3047-3051.
- [28] P. Vianello, O.A. Botrugno, A. Cappa, G. Ciossani, P. Dessanti, A. Mai, A. Mattevi, G. Meroni, S. Minucci, F. Thaler, M. Tortorici, P. Trifiro, S. Valente, M. Villa, M. Varasi, C. Mercurio, Synthesis, biological activity and mechanistic insights of 1-substituted cyclopropylamine derivatives: a novel class of irreversible inhibitors of histone demethylase KDM1A, *Eur J Med Chem*, 86 (2014) 352-363.
- [29] P. Vianello, O.A. Botrugno, A. Cappa, R. Dal Zuffo, P. Dessanti, A. Mai, B. Marrocco, A. Mattevi, G. Meroni, S. Minucci, G. Stazi, F. Thaler, P. Trifiro, S. Valente, M. Villa, M. Varasi, C. Mercurio, Discovery of a Novel Inhibitor of Histone Lysine-Specific Demethylase 1A (KDM1A/LSD1) as Orally Active Antitumor Agent, *J Med Chem*, 59 (2016) 1501-1517.

- [30] S. Miyamura, M. Araki, Y. Ota, Y. Itoh, S. Yasuda, M. Masuda, T. Taniguchi, Y. Sowa, T. Sakai, T. Suzuki, K. Itami, J. Yamaguchi, C-H activation enables a rapid structure-activity relationship study of arylcyclopropyl amines for potent and selective LSD1 inhibitors, *Org Biomol Chem*, 14 (2016) 8576-8585.
- [31] Phase I Dose Escalation Study for GSK2879552 in Subjects with Acute Myeloid Leukemia (AML). ClinicalTrials.gov Identifier: NCT02177812.
- [32] A phase I study of human pharmacokinetics and safety of ORY-1001, an LSD1 inhibitor, in relapsed or refractory acute leukaemia (AL). EudraCT number 2013-002447-29.
- [33] G. Stazi, C. Zwergel, S. Valente, A. Mai, LSD1 inhibitors: a patent review (2010-2015), *Expert Opin Ther Pat*, 26 (2016) 565-580.
- [34] R.P. Wurz, A.B. Charette, Transition metal-catalyzed cyclopropanation of alkenes in water: catalyst efficiency and in situ generation of the diazo reagent, *Org Lett*, 4 (2002) 4531-4533.
- [35] W.R. Moser, Mechanism of the copper-catalyzed addition of diazoalkanes to olefins. I. Steric effects, *Journal of the American Chemical Society*, 91 (1969) 1135-1140.
- [36] Y. Nishii, N. Maruyama, K. Wakasugi, Y. Tanabe, Synthesis and stereostructure-activity relationship of three asymmetric center pyrethroids: 2-methyl-3-phenylcyclopropylmethyl 3-phenoxybenzyl ether and cyanohydrin ester, *Bioorg Med Chem*, 9 (2001) 33-39.
- [37] N.O.M. Guibourt, A.; Castro-Palomino Laria, J., Phenylcyclopropylamine derivatives and their medical use, WO2010084160, (2010).
- [38] F. Wu, C. Zhou, Y. Yao, L. Wei, Z. Feng, L. Deng, Y. Song, 3-(Piperidin-4-ylmethoxy)pyridine Containing Compounds Are Potent Inhibitors of Lysine Specific Demethylase 1, *J Med Chem*, 59 (2016) 253-263.
- [39] T.B. Freedman, X. Cao, R.K. Dukor, L.A. Nafie, Absolute configuration determination of chiral molecules in the solution state using vibrational circular dichroism, *Chirality*, 15 (2003) 743-758.
- [40] S.S. Wesolowski, D.E. Pivonka, A rapid alternative to X-ray crystallography for chiral determination: Case studies of vibrational circular dichroism (VCD) to advance drug discovery projects, *Bioorganic & Medicinal Chemistry Letters*, 23 (2013) 4019-4025.
- [41] J. Barth, A.-M. Scheder, S. Mohr, S.-F. Johannes, M. Schmitt, A. Walter, M. Tosic, E. Metzger, M. Lübbert, M. Jung, H. Serve, R. Schüle, T. Berg, LSD1 Inhibition Induces Differentiation and Reduces the Frequency of Leukemia-Initiating Cells in Hoxa9/Meis1-Induced Acute Myeloid Leukemia, *Blood*, 128 (2016) 3935.
- [42] N. Sugino, M. Kawahara, G. Tatsumi, A. Kanai, H. Matsui, R. Yamamoto, Y. Nagai, S. Fujii, Y. Shimazu, M. Hishizawa, T. Inaba, A. Andoh, T. Suzuki, A. Takaori-Kondo, A novel LSD1 inhibitor NCD38 ameliorates MDS-related leukemia with complex karyotype by attenuating leukemia programs via activating super-enhancers, *Leukemia*, (2017).
- [43] T.C. Somervaille, M.L. Cleary, Identification and characterization of leukemia stem cells in murine MLL-AF9 acute myeloid leukemia, *Cancer Cell*, 10 (2006) 257-268.
- [44] Schrödinger Release 2013: QikProp, Schrödinger, LLC, New York, NY, **2013**.
- [45] M. Yang, J.C. Culhane, L.M. Szewczuk, P. Jalili, H.L. Ball, M. Machius, P.A. Cole, H. Yu, Structural basis for the inhibition of the LSD1 histone demethylase by the antidepressant trans-2-phenylcyclopropylamine, *Biochemistry*, 46 (2007) 8058-8065.
- [46] C. Binda, M. Li, F. Hubalek, N. Restelli, D.E. Edmondson, A. Mattevi, Insights into the mode of inhibition of human mitochondrial monoamine oxidase B from high-resolution crystal structures, *Proc Natl Acad Sci U S A*, 100 (2003) 9750-9755.

- [47] L. De Colibus, M. Li, C. Binda, A. Lustig, D.E. Edmondson, A. Mattevi, Three-dimensional structure of human monoamine oxidase A (MAO A): relation to the structures of rat MAO A and human MAO B, *Proc Natl Acad Sci U S A*, 102 (2005) 12684-12689.
- [48] Small-Molecule Drug Discovery Suite 2014-2: Glide, version 6.3, Schrödinger, LLC, New York, NY, **2014**.
- [49] E.M. Milczek, C. Binda, S. Rovida, A. Mattevi, D.E. Edmondson, The 'gating' residues Ile199 and Tyr326 in human monoamine oxidase B function in substrate and inhibitor recognition, *FEBS J*, 278 (2011) 4860-4869.
- [50] Y. Chen, Y. Yang, F. Wang, K. Wan, K. Yamane, Y. Zhang, M. Lei, Crystal structure of human histone lysine-specific demethylase 1 (LSD1), *Proc Natl Acad Sci U S A*, 103 (2006) 13956-13961.
- [51] M.A. Kerenyi, Z. Shao, Y.J. Hsu, G. Guo, S. Luc, K. O'Brien, Y. Fujiwara, C. Peng, M. Nguyen, S.H. Orkin, Histone demethylase Lsd1 represses hematopoietic stem and progenitor cell signatures during blood cell maturation, *Elife*, 2 (2013) e00633.
- [52] L. Jin, C.L. Hanigan, Y. Wu, W. Wang, B.H. Park, P.M. Woster, R.A. Casero, Loss of LSD1 (lysine-specific demethylase 1) suppresses growth and alters gene expression of human colon cancer cells in a p53- and DNMT1(DNA methyltransferase 1)-independent manner, *Biochem J*, 449 (2013) 459-468.
- [53] D. Martinez Molina, R. Jafari, M. Ignatushchenko, T. Seki, E.A. Larsson, C. Dan, L. Sreekumar, Y. Cao, P. Nordlund, Monitoring drug target engagement in cells and tissues using the cellular thermal shift assay, *Science*, 341 (2013) 84-87.
- [54] H.-U. Schildhaus, R. Riegel, W. Hartmann, S. Steiner, E. Wardelmann, S. Merkelbach-Bruse, S. Tanaka, H. Sonobe, R. Schüle, R. Buettner, J. Kirfel, Lysine-specific demethylase 1 is highly expressed in solitary fibrous tumors, synovial sarcomas, rhabdomyosarcomas, desmoplastic small round cell tumors, and malignant peripheral nerve sheath tumors, *Human Pathology*, 42 (2011) 1667-1675.
- [55] I.M. Bennani-Baiti, I. Machado, A. Llombart-Bosch, H. Kovar, Lysine-specific demethylase 1 (LSD1/KDM1A/AOF2/BHC110) is expressed and is an epigenetic drug target in chondrosarcoma, Ewing's sarcoma, osteosarcoma, and rhabdomyosarcoma, *Human Pathology*, 43 (2012) 1300-1307.
- [56] T. Haydn, E. Metzger, R. Schuele, S. Fulda, Concomitant epigenetic targeting of LSD1 and HDAC synergistically induces mitochondrial apoptosis in rhabdomyosarcoma cells, *Cell Death Dis*, (*in press*) (2017).
- [57] J.T. Lynch, M.J. Cockerill, J.R. Hitchin, D.H. Wiseman, T.C. Somerville, CD86 expression as a surrogate cellular biomarker for pharmacological inhibition of the histone demethylase lysine-specific demethylase 1, *Anal Biochem*, 442 (2013) 104-106.
- [58] P.B. Aldo, V. Craveiro, S. Guller, G. Mor, Effect of culture conditions on the phenotype of THP-1 monocyte cell line, *Am J Reprod Immunol*, 70 (2013) 80-86.
- [59] T. Maes, A.C. Buesa, Selective lsd1 and dual lsd1/mao-b inhibitors for modulating diseases associated with alterations in protein conformation, WO2012042042, (2012).
- [60] C. Buesa, C. Mascaró, D. Rotllant, C. Griñan-Ferré, M. Pallàs, T. Maes, The dual lsd1/maob inhibitor ory2001 prevents the development of the memory deficit in samp8 mice through induction of neuronal plasticity and reduction of neuroinflammation, *Alzheimer's & Dementia: The Journal of the Alzheimer's Association*, 11 P905.

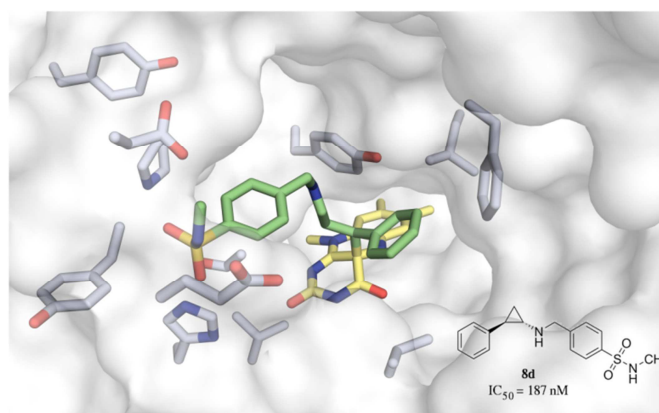
- [61] H.Y. Wey, T.M. Gilbert, N.R. Zurcher, A. She, A. Bhanot, B.D. Taillon, F.A. Schroeder, C. Wang, S.J. Haggarty, J.M. Hooker, Insights into neuroepigenetics through human histone deacetylase PET imaging, *Sci Transl Med*, 8 (2016) 351ra106.
- [62] T. Wagner, H. Greschik, T. Burgahn, K. Schmidt-kunz, A.K. Schott, J. McMillan, L. Baranauskiene, Y. Xiong, O. Fedorov, J. Jin, U. Oppermann, D. Matulis, R. Schule, M. Jung, Identification of a small-molecule ligand of the epigenetic reader protein Spindlin1 via a versatile screening platform, *Nucleic Acids Res*, 44 (2016) e88.
- [63] J.P. McGrath, K.E. Williamson, S. Balasubramanian, S. Odate, S. Arora, C. Hatton, T.M. Edwards, T. O'Brien, S. Magnuson, D. Stokoe, D.L. Daniels, B.M. Bryant, P. Trojer, Pharmacological Inhibition of the Histone Lysine Demethylase KDM1A Suppresses the Growth of Multiple Acute Myeloid Leukemia Subtypes, *Cancer Res*, 76 (2016) 1975-1988.
- [64] H.E. Gottlieb, V. Kotlyar, A. Nudelman, NMR Chemical Shifts of Common Laboratory Solvents as Trace Impurities, *J Org Chem*, 62 (1997) 7512-7515.
- [65] D. Willmann, S. Lim, S. Wetzel, E. Metzger, A. Jandausch, W. Wilk, M. Jung, I. Forne, A. Imhof, A. Janzer, J. Kirfel, H. Waldmann, R. Schule, R. Buettner, Impairment of prostate cancer cell growth by a selective and reversible lysine-specific demethylase 1 inhibitor, *Int J Cancer*, 131 (2012) 2704-2709.
- [66] E. Kroon, J. Kros, U. Thorsteinsdottir, S. Baban, A.M. Buchberg, G. Sauvageau, Hoxa9 transforms primary bone marrow cells through specific collaboration with Meis1a but not Pbx1b, *EMBO J*, 17 (1998) 3714-3725.
- [67] B. Argiropoulos, L. Palmqvist, E. Yung, F. Kuchenbauer, M. Heuser, L.M. Sly, A. Wan, G. Krystal, R.K. Humphries, Linkage of Meis1 leukemogenic activity to multiple downstream effectors including Trib2 and Ccl3, *Exp Hematol*, 36 (2008) 845-859.
- [68] Gaussian 09, Revision D.01, M. J. Frisch, G. W. Trucks, H. B. Schlegel, G. E. Scuseria, M. A. Robb, J. R. Cheeseman, G. Scalmani, V. Barone, B. Mennucci, G. A. Petersson, H. Nakatsuji, M. Caricato, X. Li, H. P. Hratchian, A. F. Izmaylov, J. Bloino, G. Zheng, J. L. Sonnenberg, M. Hada, M. Ehara, K. Toyota, R. Fukuda, J. Hasegawa, M. Ishida, T. Nakajima, Y. Honda, O. Kitao, H. Nakai, T. Vreven, J. A. Montgomery Jr., J. E. Peralta, F. Ogliaro, M. Bearpark, J. J. Heyd, E. Brothers, K. N. Kudin, V. N. Staroverov, R. Kobayashi, J. Normand, K. Raghavachari, A. Rendell, J. E. C. Burant, S. S. Iyengar, J. Tomasi, M. Cossi, N. Rega, N. J. Millam, M. Klene, J. E. Knox, J. B. Cross, V. Bakken, C. Adamo, J. Jaramillo, R. Gomperts, R. E. Stratmann, O. Yazyev, A. J. Austin, R. Cammi, C. Pomelli, J. W. Ochterski, R. L. Martin, K. Morokuma, V. G. Zakrzewski, G. A. Voth, P. Salvador, J. J. Dannenberg, S. Dapprich, A. D. Daniels, Ö. Farkas, J. B. Foresman, J. V. Ortiz, J. Cioslowski, and D. J. Fox, Gaussian, Inc., Wallingford CT, **2009**.
- [69] CDspecTech: Computer programs for calculating similarity measures of comparison between experimental and calculated dissymmetry factors and circular intensity differentials. <https://sites.google.com/site/cdspectech1>, version **21.7.2015**.
- [70] Molecular Operating Environment (MOE), 2014.09; Chemical Computing Group Inc., 1010 Sherbooke St. West, Suite #910, Montreal, QC, Canada, H3A 2R7, **2014**.
- [71] Schrödinger Release 2014-2: LigPrep, Schrödinger, LLC, New York, NY, **2014**.
- [72] P.C. Hawkins, A.G. Skillman, G.L. Warren, B.A. Ellingson, M.T. Stahl, Conformer generation with OMEGA: algorithm and validation using high quality structures from the Protein Databank and Cambridge Structural Database, *J Chem Inf Model*, 50 (2010) 572-584.
- [73] OMEGA 2.5.1.4: OpenEye Scientific Software, Santa Fe, NM. <http://www.eyesopen.com>. Hawkins, P.C.D.; Skillman, A.G.; Warren, G.L.; Ellingson, B.A.; Stahl, M.T.

[74] Schrödinger Release 2014-2: Schrödinger Suite 2014-2 Protein Preparation Wizard; Epik version 2.8, Schrödinger, LLC, New York, NY, 2014; Impact version 6.3, Schrödinger, LLC, New York, NY, 2014; Prime version 3.6, Schrödinger, LLC, New York, NY, **2014**.

[75] J.B. Baell, G.A. Holloway, New substructure filters for removal of pan assay interference compounds (PAINS) from screening libraries and for their exclusion in bioassays, *J Med Chem*, 53 (2010) 2719-2740.

ACCEPTED MANUSCRIPT

## Artwork



- New SARs are described for N-alkylated 2-PCPA-based LSD1 inhibitors.
- Potent and selective inhibitors show suppression of colony formation of leukemic cells.
- Cellular target engagement was shown by a CETSA assay.

ACCEPTED MANUSCRIPT